NCC3-126

$/N - 32 - TM$

/

A Thesis

Entitled

Microstrip Patch Antenna Receiving Array

Operating in the Ku Band

by

Douglas A. Walcher

as partial fulfillment of the requirements for

the Master of Science Degree in

Electrical Engineering

Advisor: Dr. Kai Fong Lee

Graduate School

The University of Toledo

June 1996·

An Abstract of

Microstrip Patch Antenna Receiving Array Operating in the Ku Band

Douglas A. Walcher

Microstrip patch antennas were first investigated from the idea that it would be highly advantageous to fabricate radiating elements (antennas) on the same dielectric substrate as RF circuitry and transmission lines. Other advantages were soon discovered to be its lightweight, low profile, conformability to shaped surfaces, and low manufacturing costs. Unfortunately, these same patches continually exhibit narrow bandwidths, wide beamwidths, and low antenna gain. This thesis will present the design and experimental results of a microstrip patch antenna receiving array operating in the Ku band. An antenna array will be designed in an attempt to improve its performance over a single patch. Most Ku band information signals are either wide band television images or narrow band data and voice channels. An attempt to improve the gain of the array by introducing parasitic patches on top of the array will also be presented in this thesis.

ACKNOWLEDGMENTS

Without the guidance and support from a number of people the completion of this thesis would not have been possible. I would first like to give a special thanks to Dr. Kai Fong Lee and Dr. Richard Q. Lee. Obviously, without their help this research would have never been initiated. Their expertise and enthusiasm during this research are greatly appreciated.

I would also like to thank certain members of the NASA Lewis Research Center in Cleveland Ohio for their overwhelming assistance and personal support. These members include; Mr. Michael Cauley, Mr. Kevin Lambert, Ms. Liz McQuaid, Mr. Robert Romanofsky, Mr. Kurt Shalkhauser, Dr. Rainee Simons, Mr. John Terry, Mr. Bruce Viergutz, Dr. Afroz Zaman, and Dr. Martin Zimmerman. I am also indebted to Dr. Francis Harackewicz from the University of Southern Illinois, for her advice on microstrip networks. A special thanks also goes out to Dr. Frank Kollarits for his engineering advice along with serving on my thesis committee. Furthermore, I would like to thank Dr. Charles Raquet, Head of the Antenna and RF Branch at NASA Lewis, and every member of his branch for their added technical support.

Finally, I would like to express my sincere gratitude to my family and close friends. If not for their encouragement and support I certainly would not have been able to finish this thesis or even complete graduate school.

TABLE OF CONTENTS

LIST OF FIGURES

LIST OF TABLES

Chapter 1

INTRODUCTION

A microstrip patch antenna is simply a conducting patch suspended above a ground plane as seen in figure 1-1. The conducting patch and the ground plane are separated by a low loss dielectric material called a substrate. The shape of the patch can be arbitrary. The most popular shapes however, are the rectangle and circle. A coaxial line or stripline can be used to carry electromagnetic energy to the patch. Regardless of which feed line is used, the energy is first carried to the region under the patch. This region acts like a resonant cavity with open circuits on all sides. At this point the energy is either reflected back along the same feed line or it leaks out and radiates into free space resulting in an antenna. The operating frequency of a microstrip antenna is determined by the dimensions of the patch, such as size and shape, as well as the thickness and dielectric constant (ε_r) of the substrate used to separate the patch and the ground plane. Generally, if the substrate is not changed, the operating frequency is lowered as the area of the patch is increased.
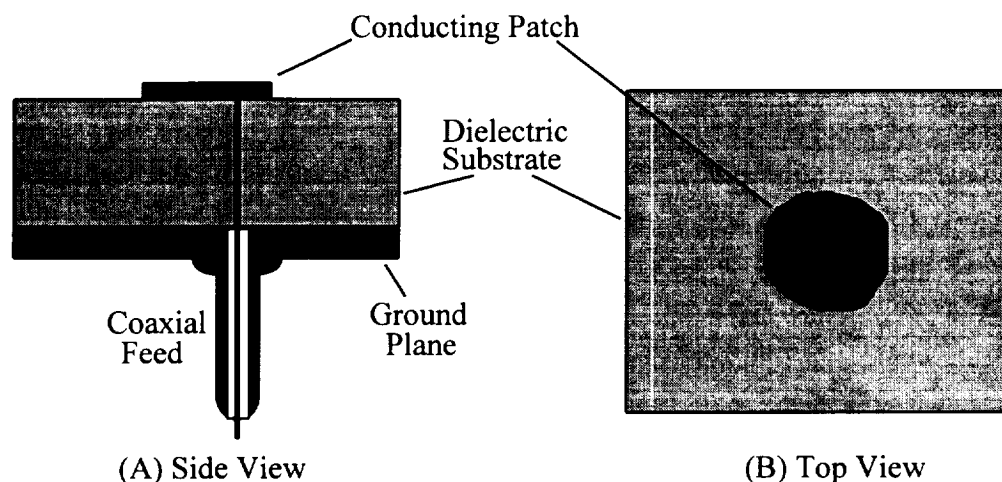
Figure 1-1. Single Microstrip Patch Antenna with Coaxial Feed
(A) Side View, (B) Top View

Microstrip antennas were first designed from the idea that it would be highly advantageous to fabricate radiating elements on the same dielectric substrate as RF circuitry and transmission lines. Other advantages of microstrip antennas were soon discovered to be its lightweight, low profile, conformability to shaped surfaces, and low manufacturing costs. High speed vehicles such as aircraft, missiles, and communication satellites are the perfect candidate for this type of antenna. Unfortunately, studies on single microstrip patches [1] have demonstrated poor antenna characteristics. Namely, single patches have exhibited narrow bandwidths, wide beamwidths, and low antenna gain.

1.1 Methods for Improving Antenna Gain, Bandwidth, and Beamwidth

Little can be done about improving the antenna characteristics of a single patch by simply changing the geometry of that patch. However, when additional patches are

placed close to a fed patch most of the antenna characteristics are improved. If the added

patches are parasitic then either the operating bandwidth of the antenna is improved or an

increase in gain is observed [2], depending on the spacing between the patches. Normally,

the gain is increased and the beamwidth is narrowed when the added patches are all fed

patches [3].

Parasitic patches can cause an increase in bandwidth by creating dual or multiple

resonances in the frequency characteristics of the antenna. They can also cause an

increase in gain by capturing and redirecting the radiation from the fed patch to enhance

the radiation in the desired broadside direction. The desired improvements will not be

sacrificed whether the parasitic patches are stacked on top of or in the same plane as the

fed patch. The stacked geometry is shown in figure 1-2 and has been called an

electromagnetically coupled patch antenna (EMCP). A coplanar geometry is shown in

figure 1-3.
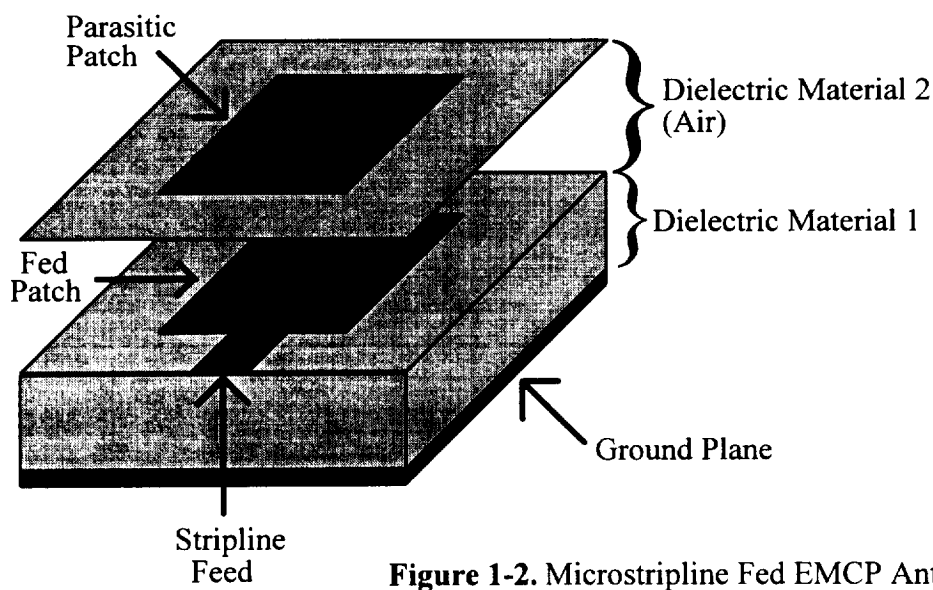
Figure 1-2. Microstripline Fed EMCP Antenna
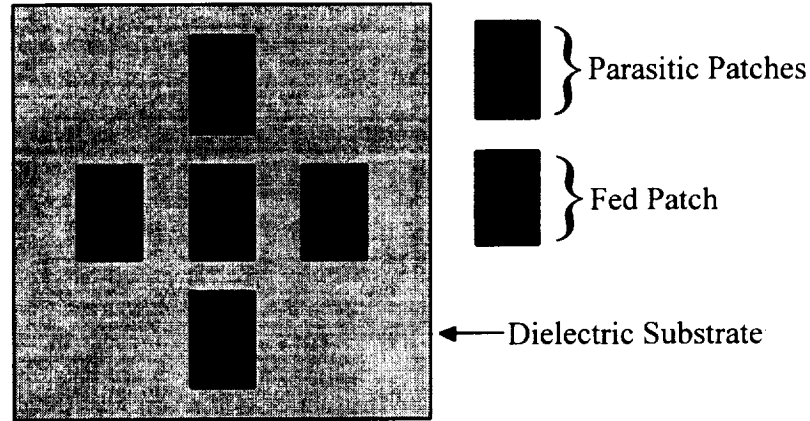
Figure 1-3. Top View of a Coplanar Cross Antenna

When two or more fed patches are placed close to one another the gain of the antenna is usually increased coinciding with a narrowing of the beamwidth. This type of arrangement is typically referred to as a microstrip patch antenna array. The most common formation of microstrip array is the planar array discussed in chapter three. A planar array exists when all the patches are placed in the same plane and are finitely spaced in two directions as seen in figure 1-4. In general, the radiation pattern of a microstrip array consists of a main beam, usually in the broadside direction, and several sidelobes. The gain is increased by focusing the radiated energy of the antenna into a narrower main beam as well as transferring energy from the sidelobes into the main beam. Typically, as the number of patches are increased so is the gain.

Still other methods have been developed that cause an increase in bandwidth without introducing additional patches. These methods increase the bandwidth of a patch by altering its substrate permittivity. A few of these permittivity altering devices may

include inserting varactor diodes or shorting posts into a patch's dielectric substrate or

creating adjustable air gaps between a patch and its ground plane.
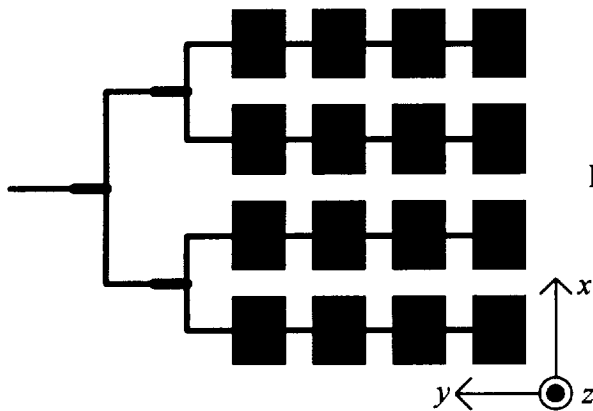
Figure 1-4. Example of a Microstrip
Planar Array Configuration

1.2 Fabrication Process

As stated before, one of the advantages of microstrip antennas is its compatibility

with integrated circuit technology. This can reduce the complexity and cost of an

electrical system in addition to reducing the power loss associated with a transition

between the antenna and printed circuit elements. The antenna patches and arrays that

were experimented on in this thesis were fabricated using a standard photo-resist-etching

process similar to the methods used to fabricate printed circuit elements.

The process, depicted in figure 1-5, works by first designing an antenna array, or

any printed circuit system, using a CAD application. Once the antenna is designed and

saved as a CAD drawing file, the file is sent to a four by eight foot Aristo plotter. The

plotter cuts the corresponding antenna pattern on a material called rubylith masking film.

Rubylith consists of a thin, clear, and somewhat rigid mylar sheet covered by a peelable

layer of soft red film [4]. A mask of the antenna is created by pealing away the red film from the areas where copper is unwanted on the circuit board. Next an unfabricated circuit board is treated with a photo-resist solution and heated. In order to eliminate the unwanted copper, the mask is placed on top of the circuit board and exposed to ultraviolet light. Areas under the red film are not exposed because it acts like a filter and blocks the ultraviolet light. The mask is then removed and the exposed circuit board is placed in a spinner where it is washed in a bath of chemicals. This spinner is only capable of spinning circuit boards smaller than 7in × 7in. Any board larger than these dimensions will fly out of the clamps when spinning has begun. The chemicals in the wash react only with exposed copper leaving the copper under the red film intact and etching away the rest. Eventually, the final product is a circuit board that is identical to the original CAD drawing. The smallest dimension that can be etched within an allowable tolerance on any circuit board has been found to be 10mils. Any dimension smaller than 10mils will be either over-etched or under-etched by an unacceptable amount.
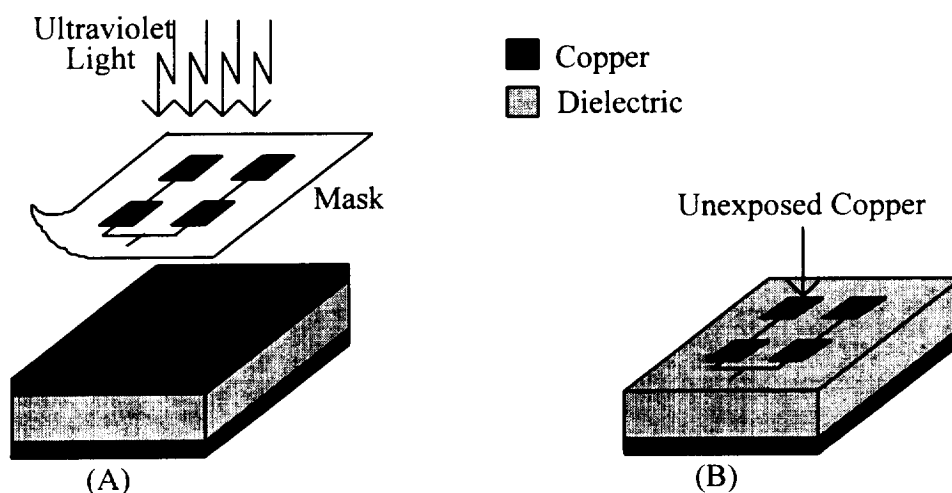
Figure 1-5. Circuit Board Fabrication (A) Before Chemical Wash and (B) After

1.3 Thesis Outline

A brief introduction to microstrip patch antennas has been presented in this chapter. Included in the introduction was a list of advantages such as compatibility with integrated circuit technology, lightweight, low profile, low cost, and pliability. Therefore, the antenna would be well suited to high speed vehicles. Some disadvantages listed were low bandwidth, high beamwidth, and low antenna gain. Methods of improving the characteristics of the antenna were then given. One method mentioned introducing parasitic patches. Another method suggested arranging a number of fed patches into an array. This thesis will present the design and experimental results of a microstrip patch antenna receiving array. The array was designed for satellite reception in the Ku band (11.7GHz - 12.7GHz). This range of frequencies was chosen due to the number of direct broadcast television satellites (DBS TV) operating in this band. Along with wide band television images, narrow band data and voice channels (radio and telephone) are also in this band.

Previous research made on microstrip antennas will be presented in chapter two. Experimental research on single patches will be given first. Research aimed at improving the characteristics of single patch antennas will then be presented. The improvements seen by each method will be given and compared with other methods.

Chapter three will begin with an introduction to the principle of pattern multiplication. This principle influences the operating characteristics of most antenna arrays. A satellite downlink power budget will then be evaluated. This power budget

will be evaluated in order to determine the amount of antenna gain required by a receiving antenna. The gain will have to be high enough in order to receive a clear television signal. The estimate for the required gain will be used to determine what size array will need to be fabricated in order to achieve the same gain. A program developed by David Pozar, called PCAAD, will be used to determine the theoretical operating characteristics of a few planar arrays. These predictions will eventually be compared with the measured results of arrays, presented in chapter five, fabricated with the same dimensions.

Preliminary experimental research conducted in this thesis is presented in chapter four. This chapter will first discuss the steps taken in the selection of a suitable substrate material. Tests were then made on single patches to optimize the dimensions of a single microstrip patch to operate in the Ku band. The chapter will then conclude with an explanation of a few research laboratories used for the completion of this thesis at the NASA Lewis Research Center in Cleveland Ohio. These laboratories were used to perform tests on the proposed arrays in order to determine their measured operating characteristics.

Chapter five will give the experimental results obtained from various tests made on the antenna arrays. Planar arrays of size 2x2, 4x4, 8x8, and finally 16x16 were tested to determine the operating characteristics for each array. The research also includes tests made on 8x8 and 16x16 arrays incorporating parasitic patches on top of the fed array layer. These tests were made to determine if an increase in antenna gain is possible without compromising the complexity of its design.

Finally, the last chapter (chapter six) will begin with a brief review of chapters one through five. The last chapter will eventually conclude with a discussion on topics of further research and possible applications of the antenna arrays presented in this thesis.

Chapter 2

PREVIOUS RESEARCH ON MICROSTRIP ANTENNAS

Chapter one briefly mentioned that research on single microstrip patch antennas has shown that they exhibit low gain, narrow bandwidths, and wide beamwidths. Up to this point the use of a single radiating patch is quite limited do to its poor operating characteristics. This chapter is intended to describe the limitations of a single patch and present some methods developed to improve these limitations.

2.1 Antenna Model

A few theoretical models have been developed in order to predict the basic characteristics (gain and bandwidth) of a single microstrip patch. The most simple of these models is known as the cavity model [5]. This model assumes the region under the radiating patch to be a resonant cavity. The cavity is bounded on the top and bottom by electric walls and on all sides by open circuit (magnetic) walls. A typical rectangular microstrip patch antenna, including dimensions, is shown in figure 2-1. If the substrate thickness (t) is much smaller than the operating wavelength, the fields under the patch can be considered transverse magnetic (TM) with the electric field perpendicular to the patch and ground plane. The electric and magnetic fields (E and H) can be determined by

solving the wave equation subject to the appropriate boundary conditions. The radiation

pattern outside the cavity can be determined from the equivalent sources on the exit

region of the cavity.
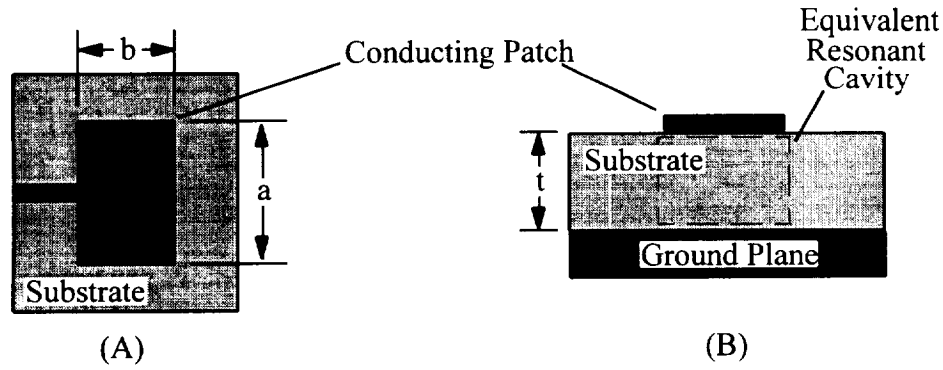
Figure 2-1.(A) Top View and (B) Side View of a Rectangular Microstrip Patch Antenna

2.2 Basic Operating Characteristics

Use of the cavity model allows easier prediction of the basic characteristics for the

microstrip patch antenna [6]. The number of resonant modes for the equivalent cavity is

infinite. The resonant frequency for each of these modes is obviously dependent on the

physical dimensions of the cavity. For instance, the size of the patch (a and b), the

dielectric permittivity of the substrate (ε_r), and the thickness of the substrate (t) can all

affect the resonant modes of the antenna. For the rectangular patch of figure 2-1 the

resonant frequencies are given by

$$f_{nm} = k_{nm}c/2\pi\sqrt{\varepsilon_r} \tag{2.1}$$

where

$$k_{nm}^2 = (m\pi/a)^2 + (n\pi/b)^2 \tag{2.2}$$

and c is the velocity of light in free space. In an effort to make the model more accurate the dimensions a and b can be substituted, in equation (2.2), for their effective dimensions to account for the presence of fringing fields. The effective dimensions are given as

$$a_e = a + t/2 \qquad (2.3)$$

$$b_e = b + t/2 . \qquad (2.4)$$

The lowest mode is usually the operating mode. For a rectangular shaped patch the lowest mode is the TM_{10}. This mode radiates strongest in the broadside direction (perpendicular to the patch). Referring to equation (2.2), as the dimensions a and b are increased each mode frequency is decreased. In other words, assuming the lowest mode is the operating mode, larger patches will have lower operating frequencies.

In an ideal situation where the ground plane under the patch is infinite, gains have been calculated to be as high as 6dB. The measured gain [6] of most patches however, is usually around 5dB, probably due to finite ground planes. The measured gain of a single patch is close to that of a quarter wave monopole which is around 4.3dB.

Referring to [1] and [5], a patch antenna simply appears as an impedance to its feeding transmission line. This impedance can change depending on the feed position between the transmission line and the patch. If the feed position is chosen carefully then a good match between the transmission line (usually 50Ω) and patch can occur. A good match is desirable in order to reduce standing waves on the transmission line which tend to degrade performance. As the applied frequency to a patch is varied from its lowest mode resonant frequency, signals can become severely degraded. In fact a patch antenna's impedance bandwidth is defined as the range of frequencies such that signal

degradation is minimal. This range is limited to the band of frequencies within which the

VSWR $\leq$ 2. Recalling from [6], the impedance bandwidth for patch antennas is

considered its operating bandwidth. The impedance bandwidth has been found to obey

the following relationship:

$$\text{Bandwidth} \propto t/\sqrt{\varepsilon_r} \, . \tag{2.5}$$

Intuitively, a very thick substrate with a low permittivity would seem to be a wise

choice for a high bandwidth antenna. However, as with any real system there is almost

always a trade-off among operating parameters. In practice, an increase in substrate

thickness causes a decrease in efficiency due to surface wave generation. Therefore, the

substrate thickness rarely exceeds $0.05\lambda_0$, where λ_0 is the free space wavelength. For a

rectangular patch the operating bandwidth usually is around 1% - 2%. To calculate a

percent bandwidth, the center frequency is divided into the difference between the upper

and lower most frequencies that fall within the VSWR $\leq$ 2 range, as shown in figure 2-2.

As a comparison, a half wave dipole has a bandwidth roughly 10% - 16% and a helical

antenna is close to 70%.
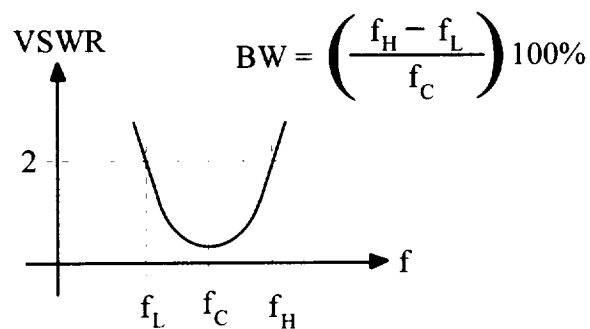
Figure 2-2. Percent Bandwidth Calculation

2.2.1 Other Patch Geometries

Up to this point the only type of patch geometry that has been mentioned is the rectangular patch. However, other geometries have also been studied [6]. The following table (table 2-1) gives a comparison of the theoretical operating characteristics between the rectangular patch and three other popular geometries. These four patches have very similar characteristics and could be used interchangeably.

Table 2-1. Comparison of basic operating characteristics for four different antenna patches (where t = 1.59mm, f = 2GHz, and ε_r = 2.32).

Characteristics	Rectangular	Circular	Equitriangular	Annular-ring
Lowest Mode	TM_{10}	TM_{11}	TM_{10}	TM_{11}
Gain, G	6.1dB	6.8dB	6.2dB	6.1dB
Directivity, D	7.0dB	7.1dB	7.1dB	7.1dB
Efficiency, η	87%	94%	87%	86%
3dB Beamwidth E-plane	102°	100°	100°	103°
H-plane	85°	80°	88°	81°
Main Beam Position	Broadside	Broadside	Broadside	Broadside
Bandwidth	0.7%	1.1%	0.8%	0.7%
Physical Area	16.1cm^2	24.3cm^2	18.1cm^2	10.6cm^2

There has been extensive research in the area of improving the bandwidth and gain of microstrip patch antennas [2], [7] - [10]. One method for improving these characteristics has been to form an array of fed patches. A similar method forms an array

by stacking parasitic patches either on top of or adjacent to a fed patch. Still other methods have included using mechanisms that slightly change the permittivity of the substrate. A review of the research in these areas is given next.

2.3 Antenna Gain Improvements

In past decades the only substantial improvements in gain, for patch antennas, have been made by combining many patches into an array. As mentioned before, an array can be built by using only fed patches or a mixture of fed and parasitic patches. However, a majority of this thesis presents research on arrays that only use fed patches. Therefore, an in depth study on these types of arrays will not be given here but in latter chapters.

Gain enhancements have been studied [7] for parasitic arrays constructed in a coplanar geometry, as illustrated in figure 2-3. This type of geometry is similar to the traditional "Yagi" TV antennas consisting of a fed dipole and one or more parasitic dipoles. Depending on the number of patches used and their interelement spacing, gains for this type of array have reached as high as 10dB for a seven element array.
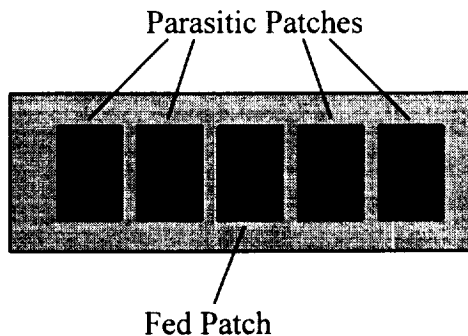
Figure 2-3. "Yagi" Type Microstrip Patch Parasitic Array

A second type of parasitic array, called an electromagnetically coupled patch antenna (EMCP), has also been studied [2], [8]. This array, shown in figure 2-4, is similar to the coplanar "Yagi" type array except that the parasitic patches are stacked on top of the fed patch. Studies on these types of antennas showed some curious results. Depending on s, the parasitic to fed patch spacing, the characteristics of the antenna could be separated into three regions. Region one experienced wide bandwidths usually exceeding 10% with gains similar to a single patch. This region occurred for s between 0 and $0.14\lambda_0$. The radiation patterns for region two $(0.15\lambda_0 \le s \le 0.30\lambda_0)$ were abnormal and this region was deemed unusable for most applications. The last region, region three $(s > 0.30\lambda_0)$, exhibited characteristics opposite those for region one. Namely, the gain was increased to 8.4dB while the bandwidth decreased back down to less than 2%.
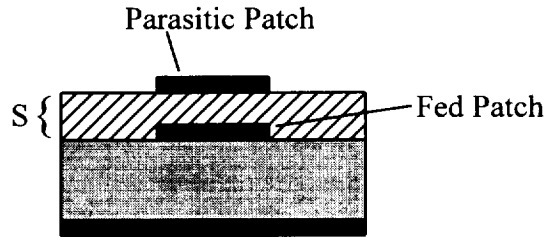
Figure 2-4. Typical EMCP Antenna

2.4 Bandwidth Improvements

As discussed in the previous section, an EMCP antenna operating in region one

can be used to create an operating bandwidth close to 10%. Another approach to

increasing the operating bandwidth of a patch is to electrically tune its impedance

bandwidth over a band of frequencies. The resonant frequency of a given patch can be

changed if the effective permittivity (ε_r) of its substrate is altered, referring to equation

(2.1). This can be accomplished by implanting either varacter diodes or shorting posts

(figure 2-5) into the dielectric substrate. A varacter diode represents a capacitance that

changes depending on its applied voltage. As the voltage applied to the diode, embedded

in the substrate changes, so does its capacitance. This ultimately changes the dielectric

permittivity [9]. Shorting posts, or switching diodes, can also alter the dielectric

permittivity by introducing an inductance into the substrate [10]. The inductance

introduced is dependent on the number of posts and their separation. Both of these

methods have obtained a tuning range around 20%.

Varacter Diode

Shorting Posts

(A)   (B)
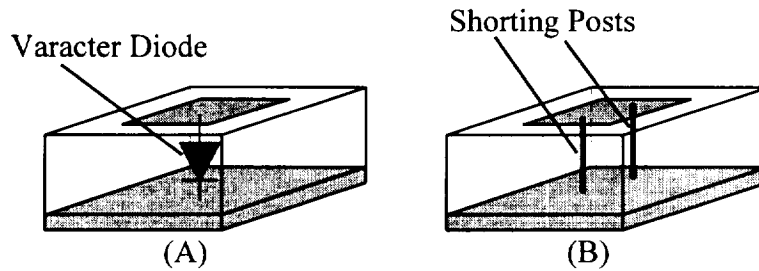
Figure 2-5. Illustrating the Use of (A) Varacter Diodes and
(B) Shorting Posts for Frequency Tuning

2.5 Chapter Summary

This chapter presented some typical operating values for a single microstrip patch

antenna. It was noted that these values were unsuitable for most applications. Therefore,

a few methods for improving these characteristics were then presented. Some of these

methods included constructing small arrays of either fed or parasitic patches. Other

methods incorporated small electrical devices such as diodes into their design. However,

it would be safe to assume that the complexity and/or size of a patch will be

compromised if its operating characteristics needed to be improved. The following table

lists comparisons of the operating characteristics between a single patch and the other

methods mentioned here.

Table 2-2. Comparison between a single microstrip patch and some other designs.

	Single Patch	2 Element EMCP Region 1	2 Element EMCP Region 3	3 Element Parasitic Array	Frequency Tunable
Gain, G	6dB	6dB	8.5dB	8.1dB	6dB
Bandwidth	1% - 2%	10% - 20%	1% - 2%	1% - 2%	$\leq 20\%$

The improved antenna methods discussed in this chapter could find some applications. However, these antennas would still be unsuitable for applications requiring very high gain ($\geq$25dB). The goal of this thesis is to construct a very high gain microstrip antenna array suitable for consumer reception of satellite television images and other satellite transmitted information. The array is to be constructed with many patches sharing the same feed line and is to operate in the Ku band (11.7GHz - 12.7GHz). The next chapter will explain the principle of pattern multiplication used to estimate the gain of an array antenna. The chapter will also include a simple power budget for a consumer satellite downlink in order to estimate the required gain of the proposed antenna array.

Chapter 3

INTRODUCTION TO ANTENNA ARRAYS

The limitations associated with a single microstrip patch have been previously mentioned in the first two chapters of this thesis. For purposes of communication with geosynchronous satellites, it is desirable to have an antenna with a very high gain and a narrow beamwidth. However, it was shown that both of these parameters were unattainable from a single patch. If an array of patches is used it would be possible to obtain a radiation pattern which is highly directive in one direction. Furthermore, as the number of elements increases the beamwidth can be made as narrow as one wishes. Intuitively speaking, the gain of an array is increased as more elements are added, because the total area of the antenna is increased. This allows more energy to be received by the antenna. The next section illustrates the principle of pattern multiplication which is used to evaluate the pattern of an antenna array. The rest of the chapter includes predicting patterns for the proposed arrays followed by the evaluation of a simple downlink power budget. The power budget will be used to predict the required receiving antenna gain needed for use in a DBS satellite downlink.

3.1 Principle of Pattern Multiplication

Suppose a typical antenna is located at some point in free space as shown in figure 3-1 [11]. Its far field representation would then be

$$E_i(\theta,\phi) = f(\theta,\phi)I_i e^{j(kr_i \cos\psi_i + \alpha_i)},$$
(3.1)

where $f(\theta,\phi)$ is the far field function of the particular antenna element in question, $k = 2\pi/\lambda_o$, I_i and α_i refers to the amplitude and phase of each element's feed current, (r_i, θ_i, ϕ_i) identifies the location of the antenna element and

$$\cos\psi_i = \cos\theta\cos\theta_i + \sin\theta\sin\theta_i \cos(\phi - \phi_i).$$
(3.2)
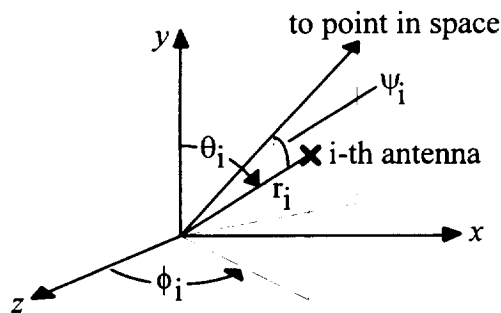
Figure 3-1. Any Antenna Element in Free Space

3.1.1 Linear Arrays

Now, suppose n identical and similarly oriented elements are situated such that they form a linear array, shown in figure 3-2. From superposition we can say that the total far field contribution would be

$$E(\theta,\phi) = E_1(\theta,\phi) + E_2(\theta,\phi) + \cdots + E_n(\theta,\phi) = \sum_{i=1}^{n} E_i(\theta,\phi),$$
(3.3)

or

$$E(\theta,\phi) = f(\theta,\phi) \sum_{i=1}^{n} I_i e^{j(kr_i \cos\psi_i + \alpha_i)} . \qquad (3.4)$$

The far field radiation pattern of the antenna array is found by taking the magnitude of

(3.4); which is,

$$|E(\theta,\phi)| = |f(\theta,\phi)| \cdot |AF| , \qquad (3.5)$$

where

$$AF = \sum_{i=1}^{n} I_i e^{j(kr_i \cos\psi_i + \alpha_i)} . \qquad (3.6)$$

The last term (AF) is usually called the array factor. It is a function of the number of

elements, the interelement spacing, and the amplitude and phase of the excitation currents

of each element. You will notice from equation (3.5) that the radiation pattern of an array

is simply the product of the individual pattern, $|f(\theta,\phi)|$, and the array factor. This

equation represents the principle of pattern multiplication. If an array is made from

hypothetical isotropic radiators, whose individual pattern is unity ($|f(\theta,\phi)\text{isotropic}| = 1$),

then the pattern will simply be the array factor.
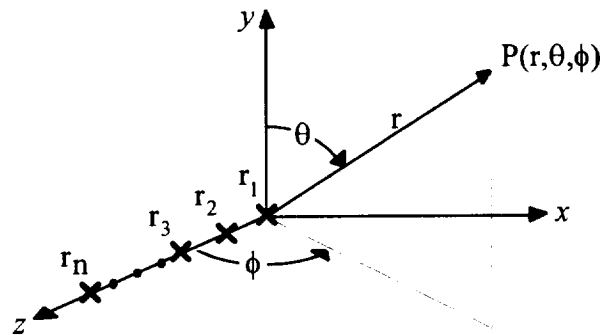
Figure 3-2. Linear Array of n Elements Along the z Axis

3.1.2 Planar Arrays

Now consider a two dimensional array situated in the x/y plane as illustrated in figure 3-3. Assuming that all of the elements are the same, it can be shown [12] that the total electric field from the array (at a distant point P) can be written as

$$E(\theta,\phi) = f(\theta,\phi)AF_x AF_y .$$ (3.7)

Again, the total radiation pattern of the array can be considered as the product of $f(\theta,\phi)$ (the individual elemental pattern), and both linear array factors, AF_x and AF_y. These linear array factors are dependent on the number of elements along the x and y axes, respectively, in addition to each element's amplitude (I) and phase (α). Stated differently, the principle of pattern multiplication also applies to two dimensional arrays.
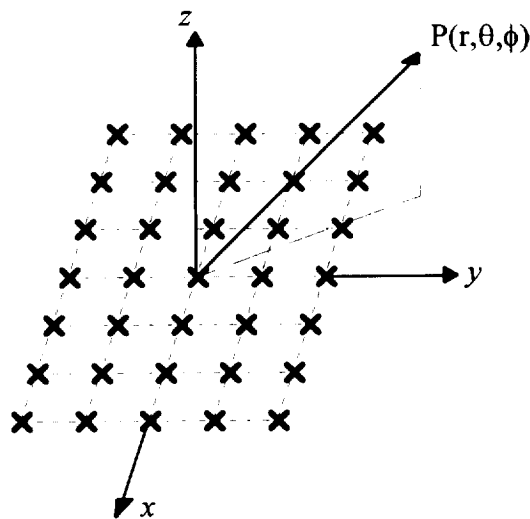
Figure 3-3. A Typical Planar Array

Determining the radiation pattern for a single antenna element is typically time consuming. Depending on the element in question, a radiation pattern calculation can also be difficult. Adding an array factor pattern makes the total radiation pattern calculation very time consuming and sometimes impossible. Therefore, many computer programs exist to aid in the design of antenna arrays. The program used extensively in this thesis was written by David Pozar and it is called PCAAD. Figures 3-4(A), 3-4(B), and 3-4(C) illustrate the difficulties in determining a radiation pattern for an array. Figure 3-4(A) is a typical pattern for a single full wave dipole. Remembering that an array of isotropic radiators is simply the pattern of an array factor, figure 3-4(B) is the array factor pattern for a uniformly spaced six element linear array. Finally, figure 3-4(C) shows the product of the two previous figures for one plane only. Again, these three figures were made using PCAAD.
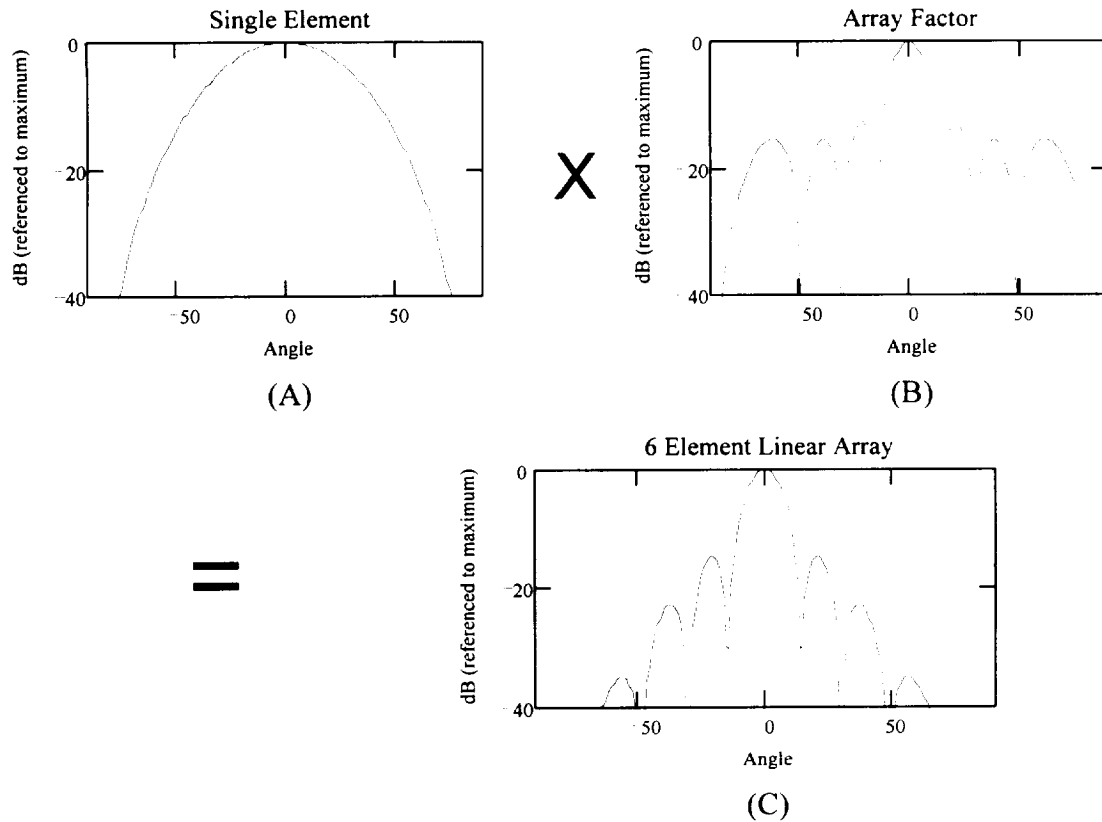
Figure 3-4 Principle of Pattern Multiplication for a Linear Array of 6 Full Wave Dipoles

3.2 Friis Power Transmission Formula

In order to determine a typical gain necessary for a receiving antenna, a DBS satellite downlink power budget will be analyzed. A downlink power budget is typically evaluated using the Friis transmission formula. There are essentially two types of communications systems: a guided wave system and a radio link. A guided wave system transmits a signal over a confined low loss structure, such as a coaxial cable or waveguide. Conversely, a radio link transmits a signal through free space. In a guided structure the power level is decayed exponentially where as the power loss in a radio link

is inversely proportional to the square of the distance. Therefore, a radio link is favorable, and sometimes necessary, for large distances. This makes antennas an important part of some communications systems.

A simplified radio link is shown in figure 3-3. Suppose the known quantities of the link are: the transmitter power (P_t), the transmit and receive antenna gains $(G_t \text{ and } G_r)$, and R the distance between them. The unknown quantity is P_r, the received power.
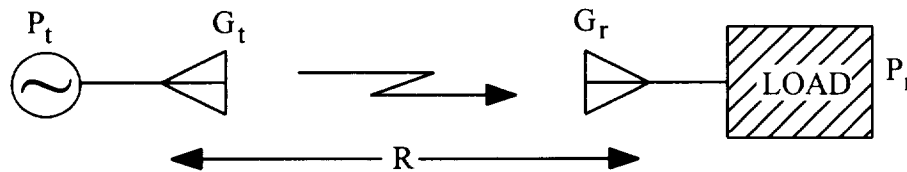
Figure 3-5. Typical Radio Link

According to [13] the power flux density incident on the receiving antenna is

$$F = \frac{P_t G_t}{4\pi R^2} \qquad \text{(Watts / meter}^2\text{)}. \qquad (3.8)$$

The total power collected by the receiving antenna is then

$$P_r = F \cdot \eta_a A \qquad \text{(Watts)}. \qquad (3.9)$$

Combining (3.8) and (3.9) we get an expression for the received power,

$$P_r = \frac{P_t G_t \eta_a A}{4\pi R^2} \qquad \text{(Watts)}. \qquad (3.10)$$

According to [7] the gain of a receiving antenna is related to its effective aperture area and can be written

$$G_{receive} = \frac{4\pi\eta_a A}{\lambda^2},$$

(3.11)

where λ is its operating wavelength. If (3.11) is substituted for the effective aperture area $(\eta_a A)$ in (3.10) then the received power can be written in terms of the parameters shown in figure 3-5. This equation is

$$P_r = P_t G_t G_r \left(\frac{\lambda}{4\pi R} \right)^2 \text{(Watts)}$$

(3.12)

and it is known as the Friis power transmission equation. The squared term is referred to as the path loss. This loss is due to the effects of the spread of energy as an electromagnetic wave travels away from a source. Therefore, this equation only represents an idealized case and does not include losses such as atmospheric attenuation, polarization mismatches, or alignment mismatches.

3.3 Downlink Power Budget

As mentioned in the previous section the Friis power transmission equation (3.12) only represents an idealized case and does not include physical power losses present in any real system. Equation (3.12) will now be rewritten to include these losses;

$$P_r = \frac{P_t G_t G_r}{Losses} \cdot \left(\frac{\lambda}{4\pi R} \right)^2,$$

(3.13)

or written in decibel terms [13];

$$P_r = EIRP + G_r - L_p - Losses \text{ (dBW)},$$

(3.14)

where EIRP is commonly called the *effective isotropically radiated power* and it is equal

to the transmitted power multiplied by antenna gain ($P_t G_t$), L_p is the path loss, and dBW

is a decibel relative to 1 Watt. The transmission formula now includes other losses but it

does not include signal degradation due to thermal noise interference generated by the

microwave devices common in any satellite link.

3.3.1 Thermal Noise

Electrical noise is generated by all active and passive microwave devices that

have a physical temperature greater than 0K. A typical communications receiver, shown

in figure 3-6(A), is made up of the receiving antenna, a demodulator (information sink),

and a few microwave devices in between. When a signal is sent from the satellite to the

receiving antenna a noise power is also added. As the signal plus noise travels from the

antenna to the demodulator each device amplifies (or attenuates) the signal as well as the

noise. However, each device also adds an additional amount of self generated noise.

Finally, at the input to the demodulator the noise power is given as [14]

$$P_n = kT_sBG, \tag{3.15}$$

where k is Boltzmann's constant which is equal to -228.6dBW/K/Hz, T_s (figure 3-6(B)) is

the equivalent noise temperature of the entire system in Kelvins, B is the system's

bandwidth in hertz, and G is the total gain of the system. A typical DBS receiving system

will have a noise temperature around 480K [15]. However, more expensive receivers will

have a lower temperature where as the opposite is also true.
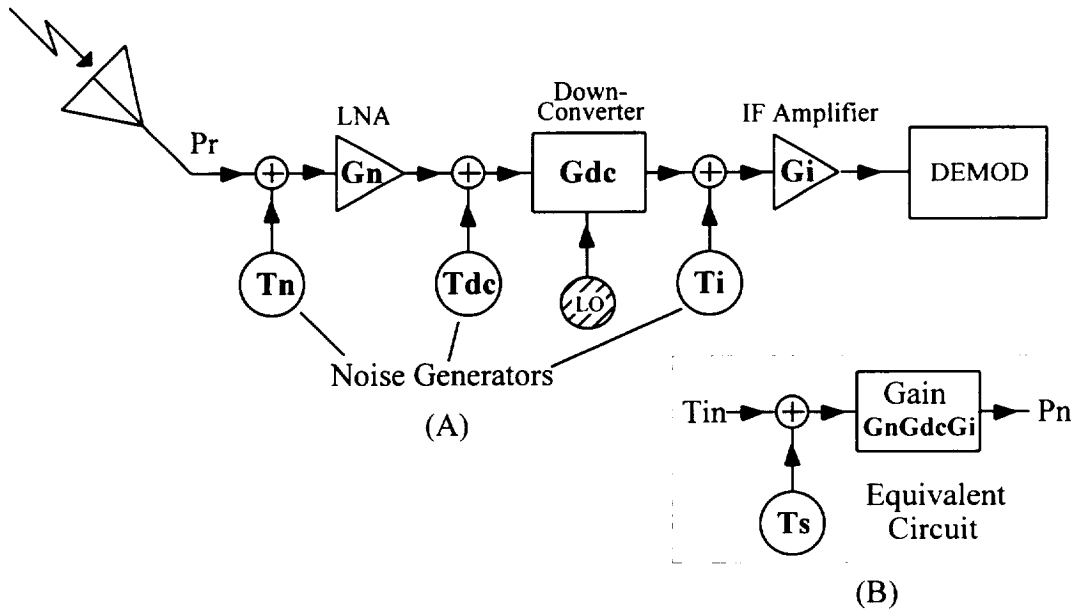
Figure 3-6. (A) Typical Communications Receiver with (B) Equivalent Circuit

In order to make an assessment as to the clarity of the received signal it must be

compared to the noise power. This is usually given as the ratio between the signal

(carrier) power over the noise power, called the carrier to noise ratio (C/N) and it is given

as

$$\frac{C}{N} = \frac{P_r G}{P_n} = \frac{P_r G}{kT_s BG} = \frac{P_r}{kT_s B}.$$

(3.16)

An acceptable carrier to noise ratio for television viewing is around 9dB [16].

Combining equations (3.14) and (3.16) and solving for the receiving antenna gain, in

decibels, we have

$$G_r = C/N - EIRP + L_p + Losses + k + T_s + B \quad (dB).$$

(3.17)

The following table is a list of a typical DBS downlink power budget. The budget is used to estimate the required gain of the receiving antenna. Typical DBS satellites have an EIRP around 60dB per 24MHz channel [15].

Table 3-1. Downlink Power Budget for a Typical DBS TV System.

DBS Satellite	
200W output power per channel	23dBW
Transmit antenna gain (**G$_t$**)	37dB
Satellite **EIRP** per channel	**60dBW**
Losses	
Path loss (**L$_p$**) at 38,000km	-205.6dB
Additional losses	-4dB
Total Losses	**-209.6dB**
Noise Power Budget	
Boltzmann's constant	-228.6dBW/K/Hz
Rx system noise temperature (**T$_s$** = 480K)	26.8dBK
Channel Bandwidth (**B** = 24MHz)	73.8dBHz
Noise Power	**-128dBW**
Required **C/N**	**9dB**
Required **G$_r$** (9 - 60 + 209.6 - 128)dB	***30.6dB***

Therefore, for a typical DBS system the receiving antenna should have a gain of at least 30.6dB in order to receive a satisfactory signal.

3.4 Predicted Array Patterns

This section will show the theoretical radiation patterns found from the program PCAAD for the proposed antenna arrays. These arrays include a 2x2, 4x4, 8x8, and 16x16 arrays. Along with pattern prediction, PCAAD can also predict the theoretical directivity for each array. In order to estimate the gain of each array an antenna efficiency, given in section 2.2, will be multiplied by the directivity. Rectangular patches will be used to construct each array and these patches have an efficiency around 85%. Another way to estimate the gain of each array is to consider that every time the physical area is doubled the gain will also be doubled or increased by 3dB. It was mentioned in section 2.2 that a single patch has a gain of roughly 5dB. Therefore, a 2x1 array (2 patches) has double the area over a single patch and would have a gain of 8dB. Furthermore, a 2x2 array (4 patches) is four times the size and would then have a gain of 11dB. Following in this fashion, the gain of a 4x4 array would be 17dB, an 8x8 array would be 23dB, and finally a 16x16 array would have an estimated gain close to 29dB, which is very close to the required 30.6dB.

The dimensions of a rectangular patch will need to be determined before any array can be constructed. The experimental procedure used to pick these dimensions will be discussed in chapter four and will not be given here. For a patch designed to operate in the Ku band the best dimensions were found, from chapter four, to be $462 \times 308 \text{ mil}^2$ ($1.17 \times 0.782 \text{ cm}^2$). The interelement spacing was chosen so that the amount of available space between patches was maximized while the radiation pattern's sidelobe levels were below a respectable level ($< -15\text{dB}$).

3.4.1 The 2x2 Array

The theoretical E-plane and H-plane patterns for the 2x2 array are shown in figures 3-7(A) and 3-7(B), respectively. From PCAAD, the directivity was estimated at 13.88dB. Therefore, multiplying by the estimated efficiency (85%), the gain can be estimated at 11.8dB. The 3dB beamwidth can also be estimated from the two figures. For the 2x2 array the beamwidth appears to be close to 40° in the E-plane and slightly less in the H-plane.

3.4.2 The 4x4 Array

Figures 3-8(A) and 3-8(B) show the patterns for the 4x4 array with a predicted directivity of 19.63dB. This translates to a gain of 16.7dB. In both the E-plane and H-plane the beamwidth appears close to 20°.

3.4.3 The 8x8 Array

The patch dimensions for the 8x8 and 16x16 arrays were enlarged to 498×332 mil^2 (1.26×0.843 cm^2). The reasons for this enlargement will be explained in chapter five, section 5.3. The patterns for this array are shown in figures 3-9(A) and 3-9(B). The directivity was estimated at 25.63dB for a gain of 21.8dB. The beamwidth for this array seems close to 15° in both planes.

3.4.4 The 16x16 Array

Finally, the patterns for the 16x16 array are shown in figures 3-10(A) and 3-10(B). This array has an estimated beamwidth around 8° in both planes. The directivity was estimated at 32.11dB for an antenna gain of 27.3dB. Compared to the gain value found from the downlink power budget, a 16x16 array may be suitable if care is taken to eliminate as much power loss in the link as possible.

(A) (B)
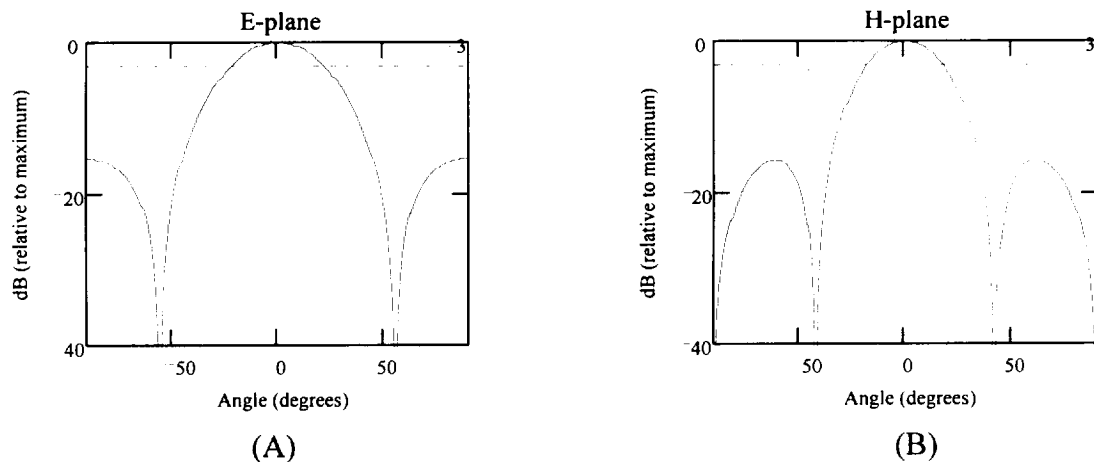
Figure 3-7. Theoretical (A) E-plane and (B) H-plane Patterns
for a 2x2 Array at 12.45GHz
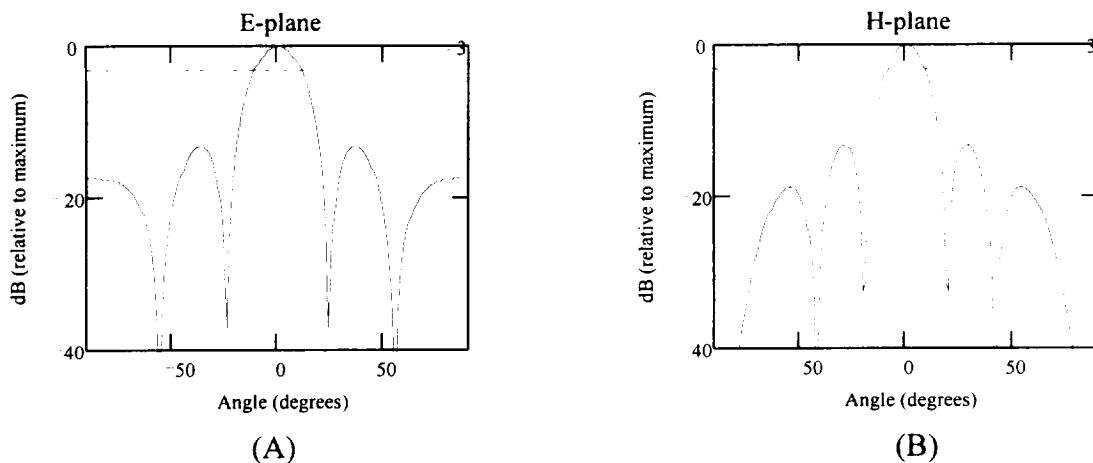
Figure 3-8 Theoretical (A) E-plane and (B) H-plane Patterns
for a 4x4 Array at 12.45GHz
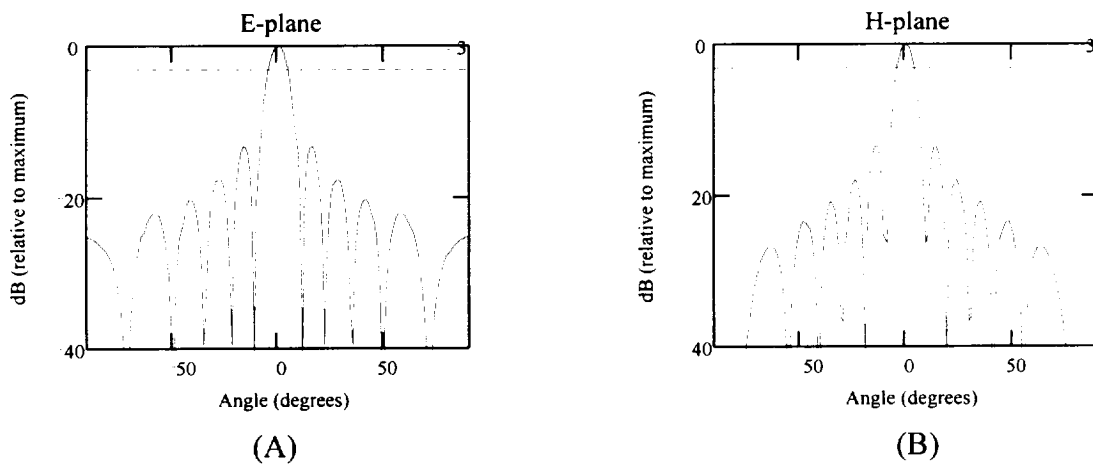
Figure 3-9. Theoretical (A) E-plane and (B) H-plane Patterns
for a 8x8 Array at 12.0GHz
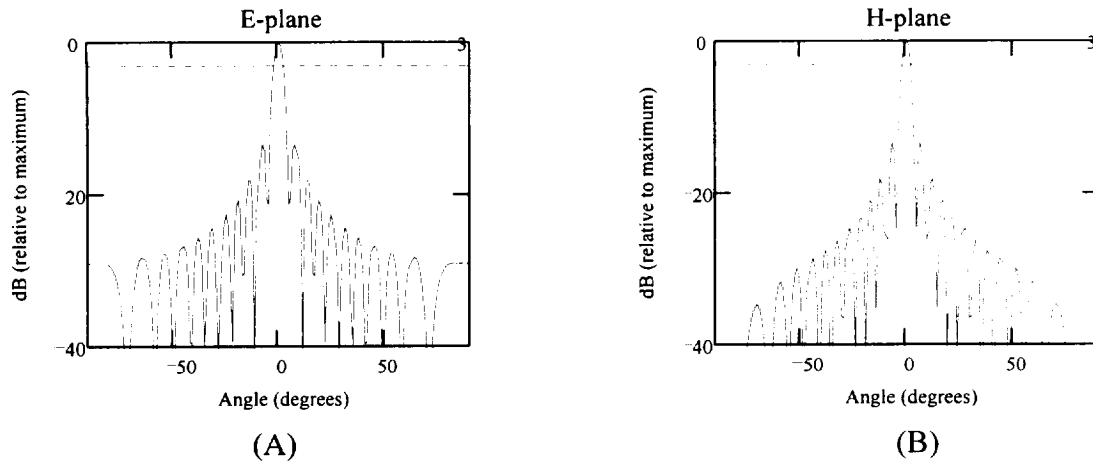
E-plane

H-plane

Figure 3-10 Theoretical (A) E-plane and (B) H-plane Patterns
for a 16x16 Array at 12.0GHz

3.5 Chapter Summary

The beginning of this chapter reviewed the principle of pattern multiplication, one

of the basic concepts used in antenna array design. This concept was explained only for a

special class of arrays known as uniform arrays. Uniform arrays consist of identical

radiating elements that are equally spaced in one (linear array) or two directions (planar

array) and are fed with currents of equal magnitude (I) and capable of having either a

uniform or progressive phase shift (α). However, our discussion was limited to arrays

with a uniform phase shift only. A uniform array with equal phase shifts will have a

pattern consisting of a single mainbeam in the broadside direction only. In general

however, the total number of elements including their interelement spacing and the

amplitude and phase of their feed currents can all affect the direction and number of mainbeams in a pattern.

Actually determining the radiation pattern of an array is usually quite difficult. Therefore, many computer programs may be used to determine these patterns. This thesis uses PCAAD in order to determine the patterns for a few planar microstrip arrays. This program was also used to estimate the gain of each array. In chapter five, experiments will be conducted on each array and their results will be compared to the predictions made in this chapter.

In an effort to judge how large a microstrip array would have to be to successfully communicate with a DBS satellite, a downlink power budget was evaluated . This budget was solved for the receiving antenna gain. It was determined that the gain would have to be above 30.6dB. However, if the user is in the center of the satellite's antenna footprint and care is taken to align the antenna properly, with an appropriate low noise receiver the gain requirement could be lessened. Therefore, comparing with the results found by the program PCAAD, a 16x16 array could possibly be used in this situation. For reasons not mentioned here but in section 5.5, an array larger than 16x16 was not fabricated and the thesis will conclude with the results for this array.

Chapter 4

EXPERIMENTAL PROCEDURES

This chapter marks the beginning of the actual design and experimental research on the proposed arrays. Before an array can be fabricated a few initial decisions must be made. The first decision should be to choose an appropriate dielectric substrate. In other words, what should be the dielectric permittivity and thickness of the substrate. The patch geometry would be decided next. Once the geometry is chosen the patch dimensions should be tuned so that they create a good match at the design frequency. Other decisions may be to decide on the type of interelement feed structure to use.

This chapter also contains information as to what type of equipment was used to conduct certain tests on these arrays. For instance, the far-field antenna testing range was used to determine the E-plane and H-plane radiation patterns of an array. In order to determine the operating bandwidth of an array, a network analyzer was used. Both of these tests were conducted using the equipment at the NASA Lewis Research Center in Cleveland, Ohio.

4.1 Substrate Selection

As stated in the introduction, before any arrays can be fabricated a suitable substrate must be chosen. The selection of a substrate is guided by many criteria. The most important criteria are, not necessarily in order:

(1) To keep the substrate thickness as thin as possible to prevent multiple surface waves;

(2) To keep the overall attenuation as low as possible;

(3) Environmental limitations, such as temperature, humidity, and aging effects;

(4) Physical limitations, such as conformability, stability, and antenna size and weight;

(5) Availability;

(6) Cost.

It was noticed that the substrate availability seemed to be the most influential criteria at NASA Lewis. The only substrates available on site were PTFE RT/duroid types 5880 and 6010 and PTFE Cuflon. The available RT/duroid 5880 (with dielectric constant, ε_r = 2.2) came in substrate thickness' of 10, 20, 25, 62, and 125 mil. Type 6010 (ε_r = 10.2) came in thickness' of 10, 25, and 50 mil. The only Cuflon (ε_r = 2.2) available came in sizes of 10 and 20 mil. However, RT/duroid 6010 was ruled out because of its relatively high loss tangent [17]. Cuflon was also ruled out because it had a tendency to curl up after etching. Therefore, the only decision left was to determine a thickness for the 5880 substrate.

4.1.1 Surface Wave Criteria

In order to eliminate multiple surface waves the substrate thickness should be made as thin as possible. However, thinner substrates cause a reduction in efficiency and operating bandwidth. Therefore, a compromise must be found. In order to determine how thick the substrate can be the following equation [18] can be used;

$$h(\text{thickness}) \leq \frac{c}{4f_u \sqrt{\varepsilon_r - 1}},$$
(4.1)

where, c is the velocity of light and f_u is the maximum operating frequency (12.7GHz). Substituting $\varepsilon_r = 2.2$ into equation (4.1) and solving, we get a maximum substrate thickness of

$$h \leq 212\text{mil (0.54cm)}.$$
(4.2)

Therefore, all of the available substrates are still suitable candidates.

4.1.2 Attenuation

Before the thickness can be chosen a few more criteria must be examined. One of these is the relationship between attenuation and substrate thickness. The attenuation constant in a microstrip circuit is given by [19]

$$\alpha = \alpha_d + \alpha_c,$$
(4.3)

where α_d is the attenuation constant due to dielectric loss and α_c is due to conductor loss. Figure 4-1 shows how the total attenuation constant varies with thickness. The full details of this dependence is not given here but is referenced in [19].

RT/duroid 5880 (Zo = 50 Ohms)
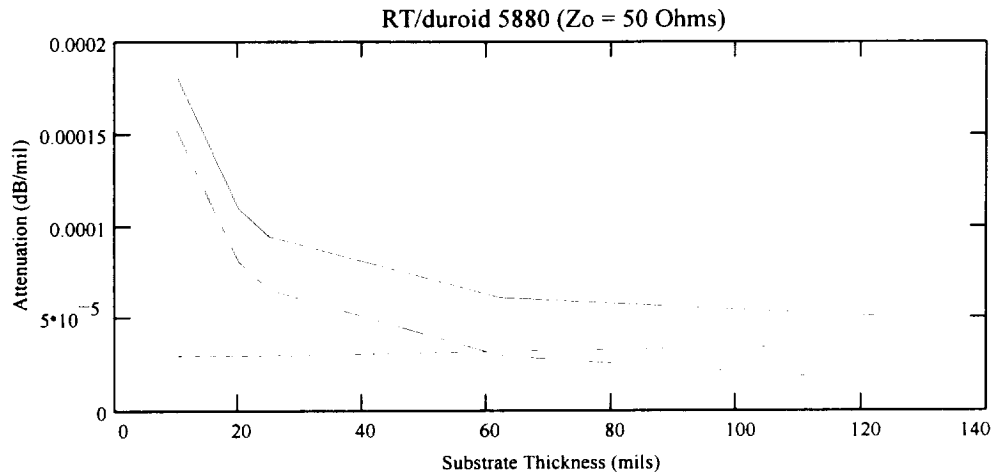
Figure 4-1 Attenuation Constant versus Substrate Thickness

$$(\text{---} \ \alpha_{total}, \ \text{----} \ \alpha_d, \ \text{---}\cdot\text{---} \ \alpha_c)$$

Figure 4-1 clearly indicates that as the thickness of the substrate is increased, the

attenuation is decreased. This should lead to concluding that the 125mil thick substrate is

the best choice. However, the size of a typical microstrip network is increased as the

thickness is increased. For instance, the width of a 50Ω transmission line is only 63mil

when the substrate thickness is 20mil. In contrast, a 62mil thick substrate increases the

transmission line width to 212mil. Remembering that in order to achieve a normal

radiation pattern, the separation between patches should be less than one free space

wavelength, which at 12GHz is roughly 980mil. Therefore, for very large substrate

thickness', arranging a number of patches into an array becomes quite difficult. With all

of these factors taken into account, the substrate eventually chosen was RT/duroid 5880

with a thickness of 20mil.

4.2 Single Patch Antennas

Once a decision was made as to which substrate would be used, experiments on single rectangular patches were finally begun. The geometry of the patch was chosen to be rectangular because of the lack of difficulty in both drawing the patch using a CAD application and cutting out its mask using a plotter. The initial dimensions of the patch were chosen so that operation would be close to 12.45GHz. This frequency was chosen because the density of higher powered DBS satellites is greater in the 12.2GHz to 12.7GHz band.

At this point it was decided that each patch would be fed via a 50Ω microstrip transmission line. If the patch is normalized to 50Ω then the interelement feed structure is easier to design when an array is eventually built. Recalling from chapter two, the impedance of a patch changes with its feed position. Therefore, referring to figure 4-2, an optimum insertion depth along with an appropriate gap dimension would have to be found in order to produce a good match between the feed line and the patch. To operate this patch close to 12.45GHz the a and b dimensions would also have to be adjusted. However, according to [20] the a to b aspect ratio should be kept to 1.5 (a/b = 1.5) in an effort to keep cross polarization levels at a minimum. Using the aspect ratio criteria and equations (2.1) and (2.2), the initial dimensions were found to be; a = 480mil (1.22cm) and b = 320mil (0.813cm) for the lowest order TM_{10} mode.

In order to determine the best set of dimensions, each patch was connected to an HP8510 Network Analyzer. A network analyzer measures the S parameters, discussed in the next section, of a one or two port network as a function of frequency. After each

antenna patch was connected, the HP8510 was set up in a one port configuration and an S_{11} parameter was measured. The S_{11} parameter in this case is basically the reflection coefficient of a particular antenna. The larger the S_{11} parameter the worse the match. Therefore, the patch that produces the lowest S_{11} value is obviously the best design.

In order to optimize the dimensions of the single patch a number of slightly different patches were fabricated and tested on the network analyzer. Two dimensions were altered in each patch. The first two dimensions optimized were the gap and depth dimensions. In order to optimize these dimensions a and b were not varied. As stated previously in this section, these dimensions were originally set to a = 480mil and b = 320mil.

The first five patches tested all had a gap of 10mil each with a depth insertion that was varied from 64mil to 80mil in steps of 4mil. The second five patches tested had a gap of 12mil for the same five depth insertions. In all, twenty five patches were tested where the gap was varied from 10mil to 18mil in steps of 2mil and the depth was varied from 64mil to 80mil in steps of 4mil. The microstrip patch that produced the best match had a gap of 10mil and a depth of 64mil.

However, this patch operated at a frequency of 12.1GHz. In order to bring the operating frequency back up to the design frequency (12.45GHz) a second group of patches were tested with changes made in the a and b dimensions followed by a change in the depth of insertion. After a number of trials a single microstrip patch with the following dimensions was found to produce the best match closest to 12.45GHz: a = 462mil (1.17cm), b = 308mil (0.782cm), d = 66mil (0.168cm), and g = 10mil (0.025cm).
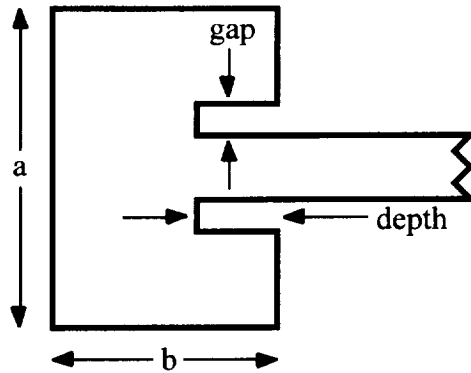
Figure 4-2. Typical Microstrip Antenna Patch with Microstripline Feed

4.3 Impedance Bandwidth

As mentioned in the previous section, a network analyzer measures the S

parameters of a network as a function of frequency. Each S parameter in the scattering

matrix of an *n* port microwave network can be defined in terms of a voltage wave

incident on that port (V_n^+) and the corresponding voltage wave reflected back (V_n^-). In

terms of these incident and reflected waves the matrix is defined as [21]

$$\begin{bmatrix} V_1^- \\ V_2^- \\ \vdots \\ V_n^- \end{bmatrix} = \begin{bmatrix} S_{11} & S_{12} & \cdots & S_{1n} \\ S_{21} & & & \vdots \\ \vdots & & & \\ S_{n1} & \cdots & & S_{nn} \end{bmatrix} \begin{bmatrix} V_1^+ \\ V_2^+ \\ \vdots \\ V_n^+ \end{bmatrix} \tag{4.4}$$

One element from the matrix is then defined as

$$S_{ij} = \frac{V_i^-}{V_j^+}\Bigg|_{V_k^+ = 0, k \neq j} \tag{4.5}$$

In other words S_{ij} can be found by driving port j with an incident wave and measuring the wave reflected from port i while all other ports are terminated in matched loads. Therefore, the reflection coefficient of port i is the S_{ii} parameter and S_{ij} is the transmission coefficient from port j to i. If the network has only one port, as is the case with a single patch antenna, then the matrix is simply one term; the reflection coefficient (S_{11}).

When a patch is connected to the network analyzer this reflection coefficient becomes a measure of its input impedance. Usually the impedance of a patch is measured over a large band of frequencies. At certain frequencies this impedance can be larger or smaller than the desired 50Ω. If the deviation is very large then standing waves will occur and the signal becomes deteriorated. The impedance bandwidth is therefore defined as the band of frequencies such that signal degradation is minimal, or when the VSWR ≤ 2. For the purposes of this thesis it was more convenient to define the bandwidth as the band of frequencies such that $S_{11} \leq -10\text{dB}$ (VSWR ≤ 1.22). Under the following criteria the bandwidth of the single patch was determined to be close to 2.5%.

4.4 Antenna Gain and Radiation Pattern Measurements

The gain and pattern measurements for all of the arrays investigated in this thesis were conducted at the far field antenna measurement facility at NASA Lewis. The current configuration is shown in figure 4-3. This system was developed by John Terry formally of NASA Lewis.
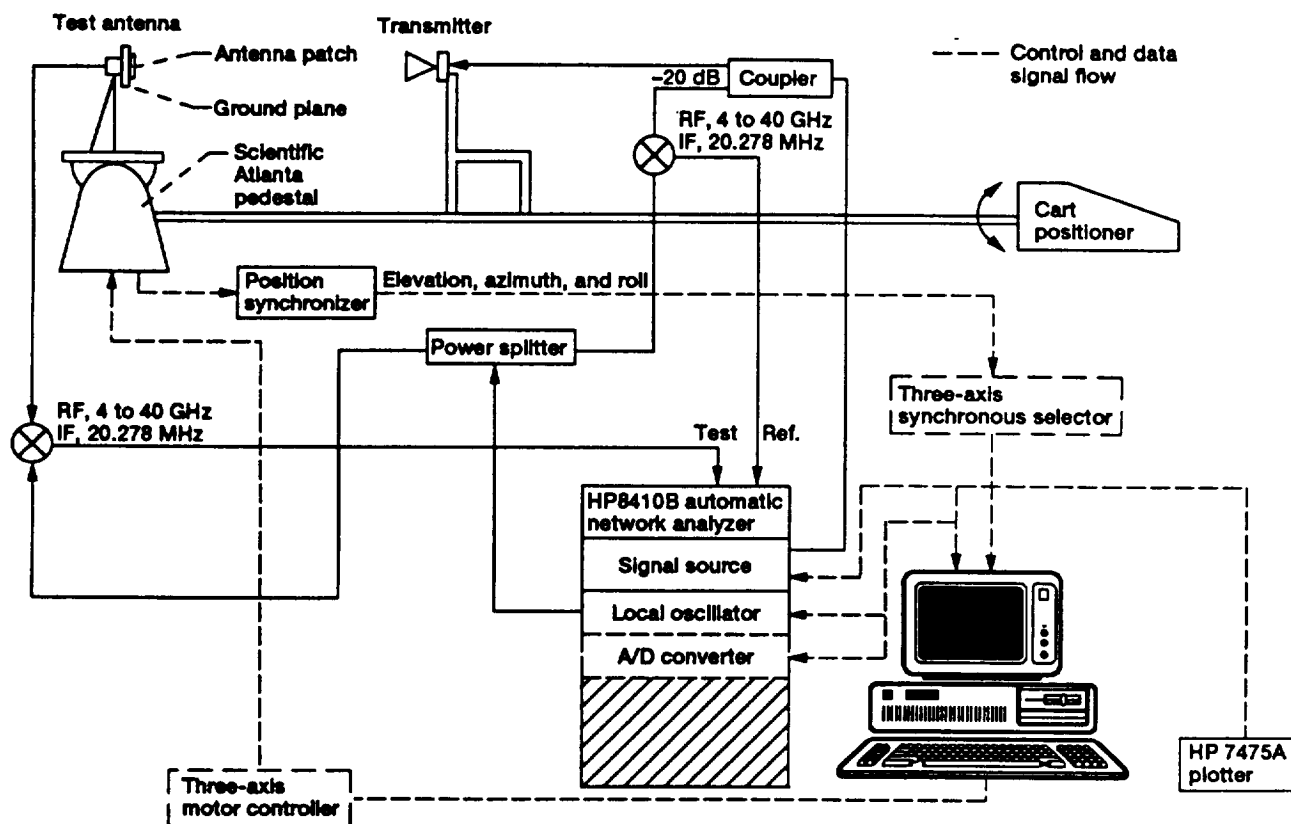
Figure 4-3. NASA Lewis Research Center Far Field Antenna
Measurement Facility Block Diagram

This facility is capable of making up to four different types of measurements:

amplitude-vs-frequency, *amplitude-vs-angle*, *phase-vs-frequency*, and *phase-vs-angle*.

The E-plane and H-plane measurements are given as amplitude-vs-angle plots (dB-vs-

degrees). The gain of an antenna can be evaluated from this measurement as well. The

bandwidth of an antenna could be determined from the amplitude-vs-frequency plot but

usually isn't because this plot is dependent on the transmitting antenna which is not a linear device with respect to frequency.

A Hewlett Packard personnel computer is used to control each measurement process. All the necessary information about which type of measurement will be made is entered into the PC. This information usually includes a frequency range, an output power level, and an angular position sweep. The PC uses this information to control the microwave transmitting hardware. A source signal is created by the transmitting hardware and is first divided in two. One part of the source signal is sent back to the receiver in order to establish a reference signal. The remaining source signal power is used to feed a calibrated transmit antenna, with known antenna gain, which is pointed in the direction of the antenna under test (AUT). The distance between the transmitting antenna and the AUT is large enough to ensure that the radiated wave is essentially a plane wave as it reaches the AUT (far field).

4.4.1 Radiation Pattern Measurement

The signal received by the AUT is sent to the receiver. To calculate a radiation pattern the AUT is mounted on a turntable whose angular position is controlled by the PC. The position of the AUT is usually rotated from -90° to 90°, where the broadside of the AUT is at 0°. The received signal and the reference signal are compared at the receiver where a corresponding amplitude and phase is assigned for each position by an HP8410B network analyzer. This information is sent back to the PC where the amplitude and phase is correlated with its correct angular position. This information can then be

presented in the form of an *x/y* plot as either an amplitude-vs-angle plot or a phase-vs-angle plot.

4.4.2 Antenna Gain Measurement

The gain of the AUT can be measured by comparing its maximum power received to the maximum power received by a standard gain horn with known antenna gain. The difference between the received maximums of the two antennas is either added or subtracted from the antenna gain of the horn and assigned to the AUT. For example, at 12GHz the maximum power received by the AUT is 20dB and by the horn is 25dB, for a difference of -5dB. At the same frequency the horn is rated at a gain of 23.6dB. Therefore, the AUT is measured to have a gain of about 18.6dB.

4.5 Chapter Summary

This chapter began by detailing the selection process used in choosing the microstrip patch substrate material. After taking stock of the available material supplied by NASA Lewis the selection process was used to weed out all the unwanted material. The material that was eventually used was RT/duroid 5880 with a dielectric thickness of 20mil and dielectric permittivity of 2.2.

The chapter then proceeded to explain what experiments were made on single patch antennas. An S parameter test was necessary to determine the best dimensions for a single patch in order to operate close to 12.45GHz. The optimized dimensions were found to be a = 462mil, b = 308mil, d = 66mil, and g = 10mil.

The chapter eventually concluded with describing the impedance bandwidth and radiation pattern measurement techniques used to evaluate all of the antenna arrays in this thesis. Furthermore, a description of the antenna gain measurement was also given. Namely, the gain of each array was measured based on its maximum power received and the antenna gain of a standard gain horn. All three of these measurement techniques can be made using equipment supplied by the NASA Lewis Research Center.

Chapter 5

EXPERIMENTAL RESULTS FOR THE ANTENNA ARRAYS

The experimental results of the 2x2, 4x4, and 8x8 sub-arrays as well as the 16x16 array will be presented in this chapter. The operating bandwidth, radiation pattern, and antenna gain will all be determined for all four of these arrays. In addition, the measured gain and radiation pattern will be compared to the predictions made in chapter three.

5.1 The 2x2 Sub-Array

The first step in the design of this array was to determine a suitable interelement feed structure. Since the bandwidth of the single patch was only 2.5%, a simple quarter wave parallel feed network was considered adequate. The feed network, shown in figure 5-1, consists of a 70.7Ω quarter wave transmission line used to transform a 50Ω antenna into a 100Ω load. Two 100Ω loads can then be combined, in parallel, to form another 50Ω load. This process can be repeated for each pair of patch antennas.
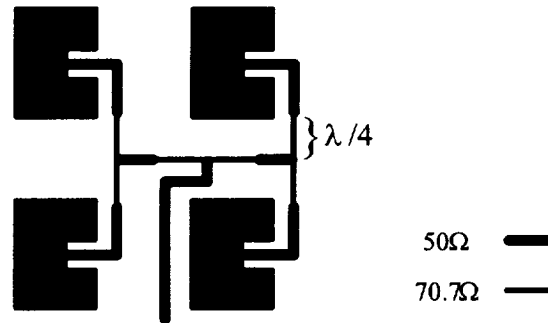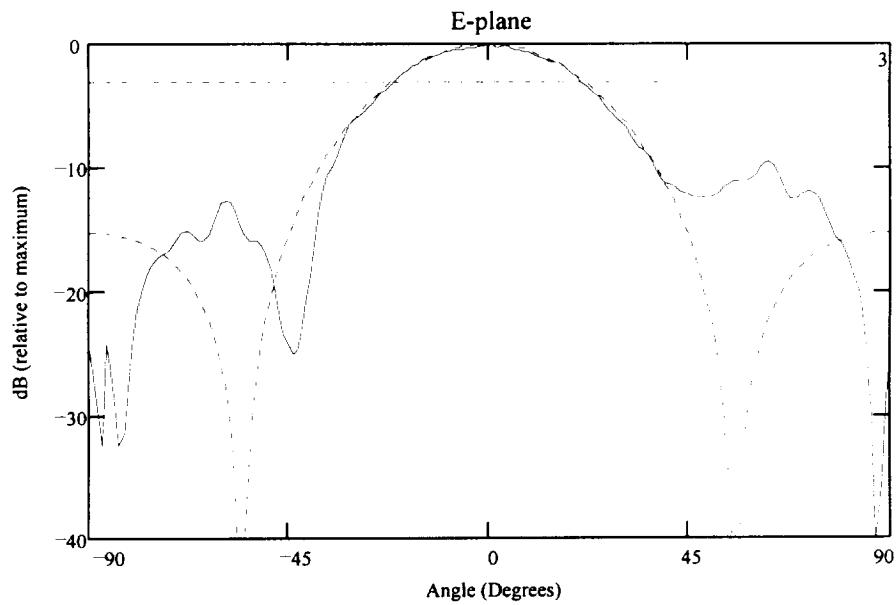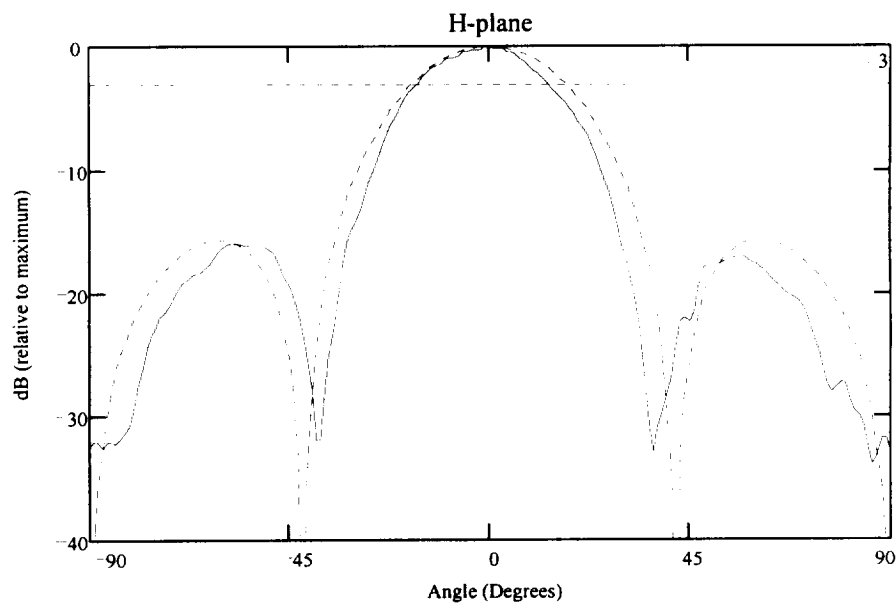
Figure 5-1. 2x2 Sub-Array Layout with Quarter Wave Transformers

5.1.1 Measured Operating Characteristics of the 2x2 Sub-Array

The measured E-plane and H-plane patterns are given in figures 5-2(A) and

5-2(B), respectively. Both patterns are shown with respect to its corresponding

theoretical pattern predicted in chapter three. The measured 3dB beamwidth is roughly

42° in the E-plane and 30° in the H-plane. The gain was calculated to be close to 11dB.

All three of these values seem to be comparable to the predicted values of chapter three.

From figure 5-3, the bandwidth is close to 2.1%, which is a reasonable value considering

the single patch bandwidth is 2.5%. However, probably due to coupling between patches,

the center frequency shifted down to 12.29GHz, slightly lower than the design frequency

of 12.45GHz.

E-plane

(A)

H-plane

(B)

Figure 5-2 (A) E-plane and (B) H-Plane Patterns
for the 2x2 Sub-Array at 12.29GHz
— Measured, ---- Theoretical

S₁₁   log MAG
REF 0.0 dB
1   10.0 dB/
▽   -18.497 dB

hp

C

MARKER 1
    12.2875 GHz

1→

1
▽

←   Ku Band ⟶

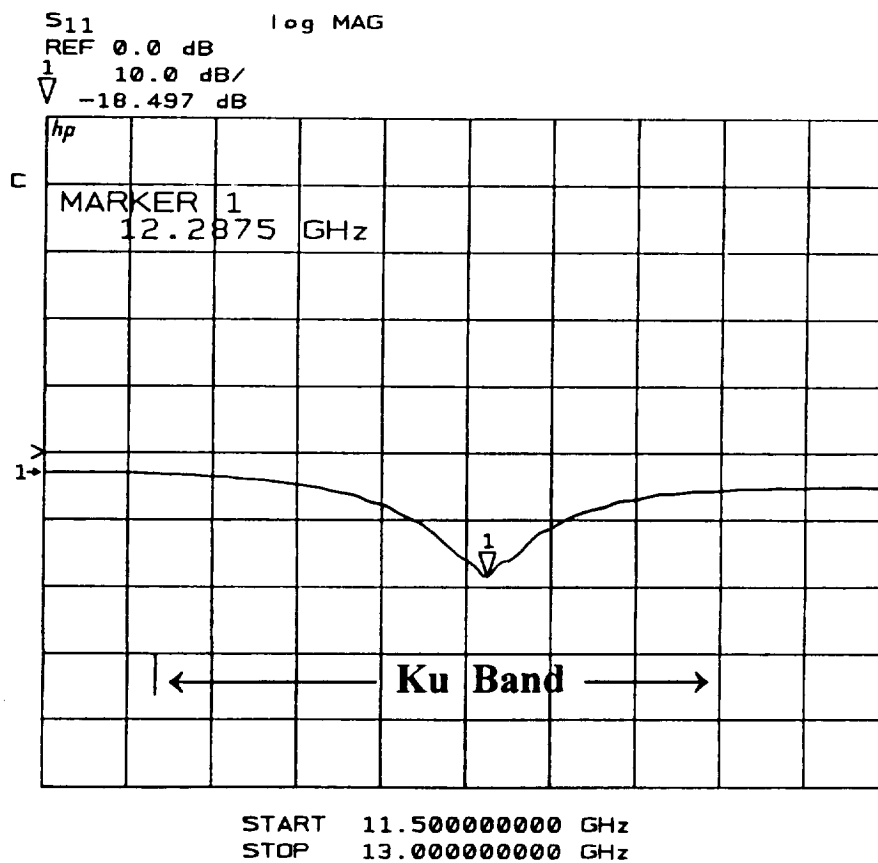START   11.500000000 GHz
STOP   13.000000000 GHz

Figure 5-3. Reflection Coefficient -vs- Frequency for the 2x2 Sub-Array

5.2 The 4x4 Sub-Array

This array was fabricated using four of the 2x2 sub-arrays mentioned in the previous section. Each patch was fed with the same interelement feed structure. The actual mask of the 4x4 sub-array is shown in figure 5-4.

5.2.1 Measured Operating Characteristics of the 4x4 Sub-Array

Figures 5-5(A) and 5-5(B) show the measured E-plane and H-plane patterns with respect to their predicted patterns. The E-plane 3dB beamwidth was determined to be roughly 20° and the H-plane beamwidth was determined to be 16°. The gain for this array was calculated to be 19dB. It appears that the nulls in both patterns match up fairly well with the nulls from the predicted patterns, indicating a normal radiation pattern. The operating bandwidth for the 4x4 sub-array, shown in figure 5-6, is also close to 2.1%. However, the center frequency of this array shifted up to 12.54GHz, slightly higher than the center frequency of the 2x2 sub-array. This frequency shift could also be attributed to coupling.
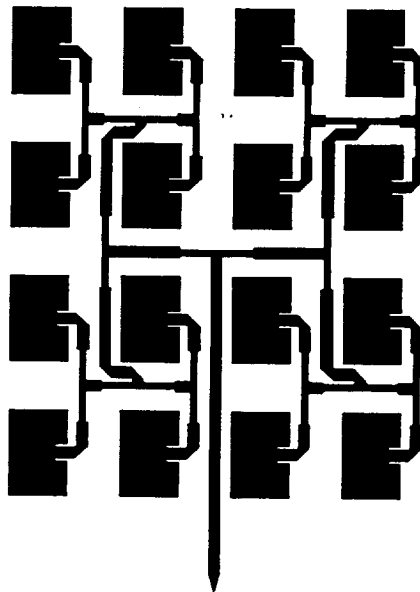
Figure 5-4. Mask of the 4x4 Sub-Array Shown Actual Size
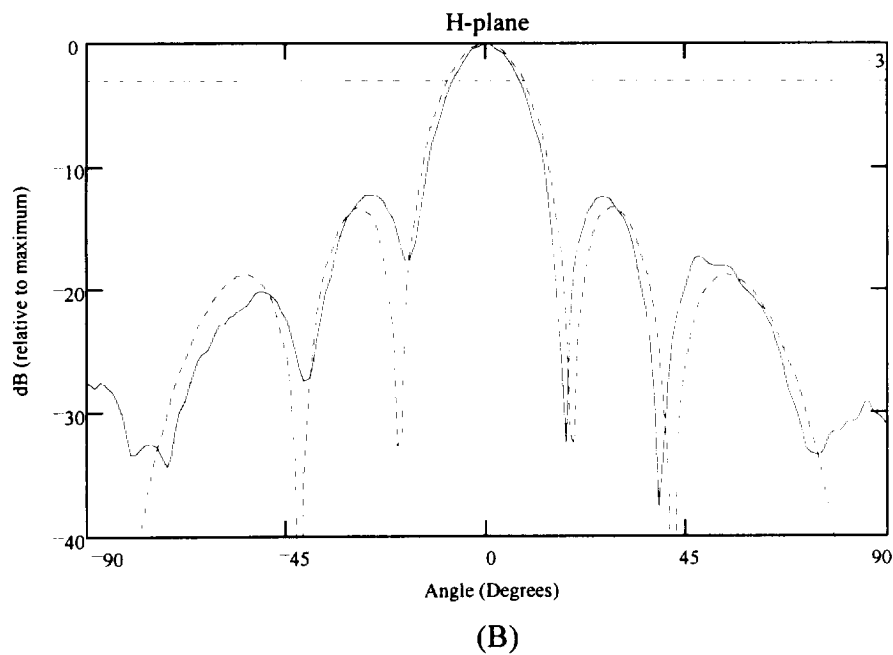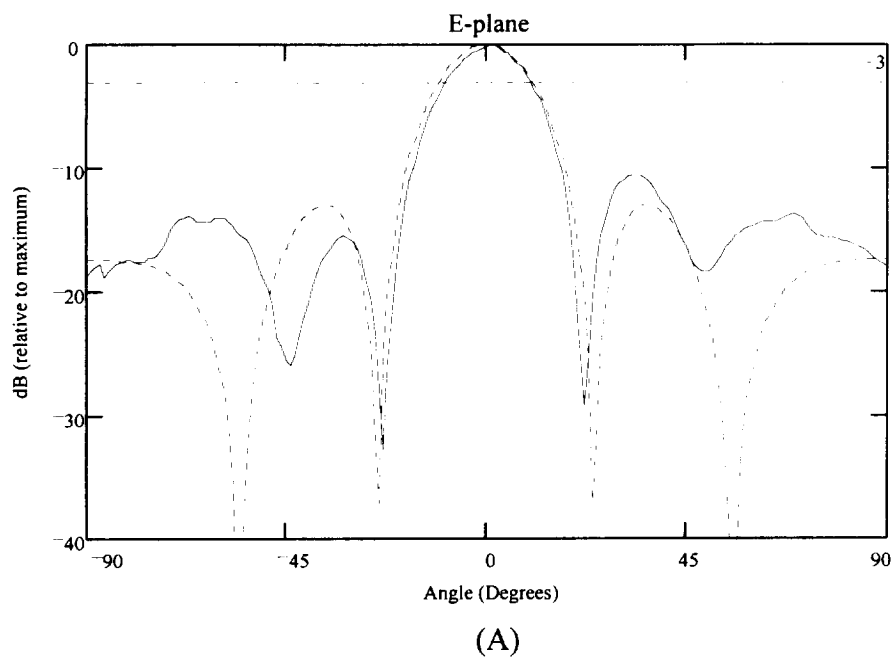
Figure 5-5. (A) E-plane and (B) H-Plane Patterns
for the 4x4 Sub-Array at 12.54GHz
— Measured, ---- Theoretical
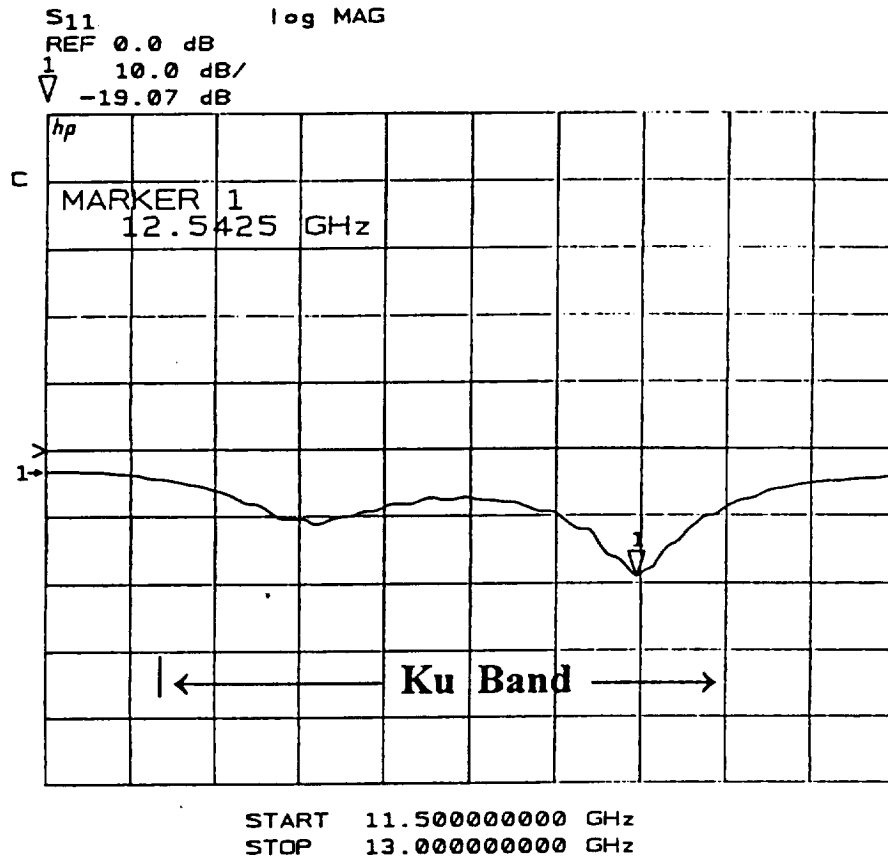
Figure 5-6. Reflection Coefficient -vs- Frequency for the 4x4 Sub-Array

5.3 The 8x8 Sub-Array

The first 8x8 sub-array fabricated was made from four of the 4x4 sub-arrays

described in section 5-2. It was mentioned in section 5.2.1 that the center frequency of

the 4x4 array experienced an upward shift with respect to the 2x2 array. This trend

continued, as illustrated in figure 5-7, when this first 8x8 sub-array was tested. In order

to bring the operating frequency back down, a second 8x8 sub-array was designed. Each

patch in this new array was enlarged according to equations (2.1), (2.2), and the aspect

ratio criteria (a/b = 1.5). About the same time in this thesis research it was discovered

that the satellite receiving equipment available at NASA Lewis operated only in the older

Ku band (11.7GHz - 12.2GHz). Therefore, the target frequency for this new 8x8 sub-
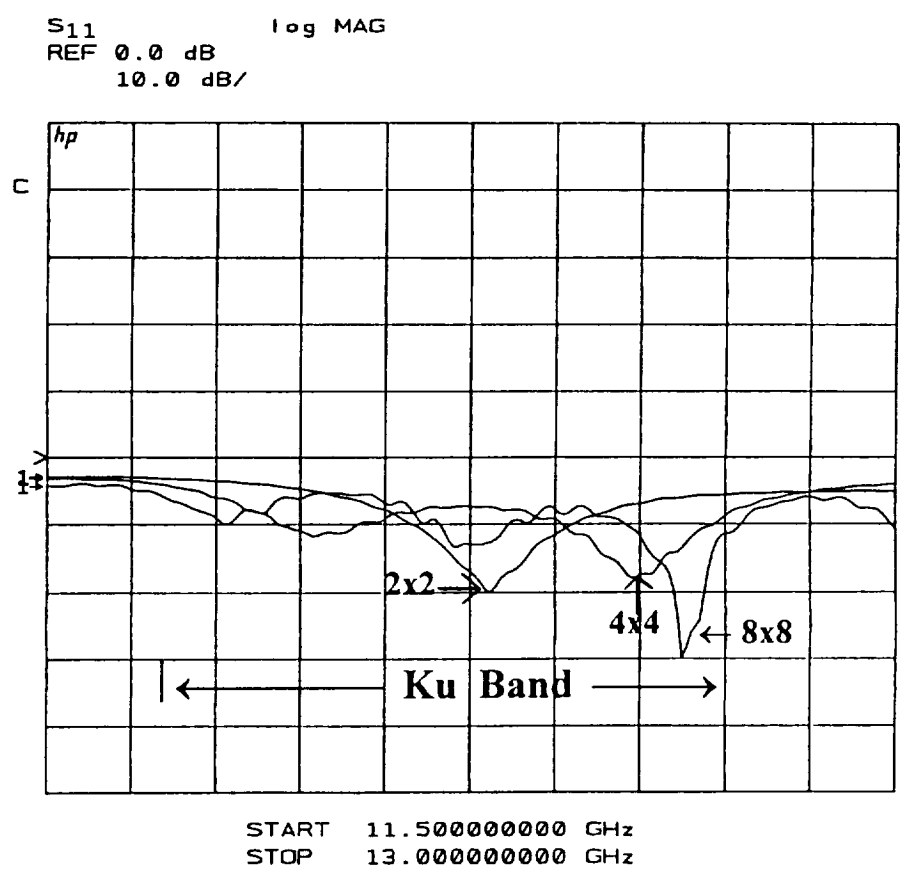
array was set at 12.0GHz instead of 12.45GHz.

S_{11} log MAG
REF 0.0 dB
    10.0 dB/

Figure 5-7. Upward Shift of the Center Frequency for the
2x2, 4x4, and 8x8 Sub-Arrays

Limited to the aspect ratio criteria, equations (2.1) and (2.2) were solved for the dimensions, a and b, at a frequency of 12GHz. These new patch dimensions were found to be a = 498mil (1.26cm) and b = 332mil (0.843cm). In order to complete the changes needed for a transformation to the lower frequency, the interelement feed structure was also modified. The adjustments needed were to appropriately lengthen each quarter wave transformer and determine a satisfactory spacing between each patch. Since the new operating wavelength is larger, the distance between patches could be increased without creating huge distortions in the radiation pattern. The mask for this modified 8x8 sub-array is shown, actual size, in figure 5-8.

5.3.1 Measured Operating Characteristics of the 8x8 Sub-Array

The E-plane and H-plane radiation patterns of the modified 8x8 sub-array are shown in figures 5-9 (A) and (B). The 3dB beamwidth was calculated to be 11° in the E-plane and closer to 9° in the H-plane. The gain was estimated to be 22.5dB at 12GHz. Again, it is evident from figures 5-9 (A) and (B) that the nulls of each pattern match up very well with the predicted patterns, indicating a normal pattern. The operating bandwidth of this sub-array is 1.3%, calculated from figure 5-10. Figure 5-11 illustrates the difference in the center frequencies of the two 8x8 sub-arrays. As one can see the modified sub-array operates close to 12GHz while the unmodified sub-array has a center frequency almost outside the Ku band.
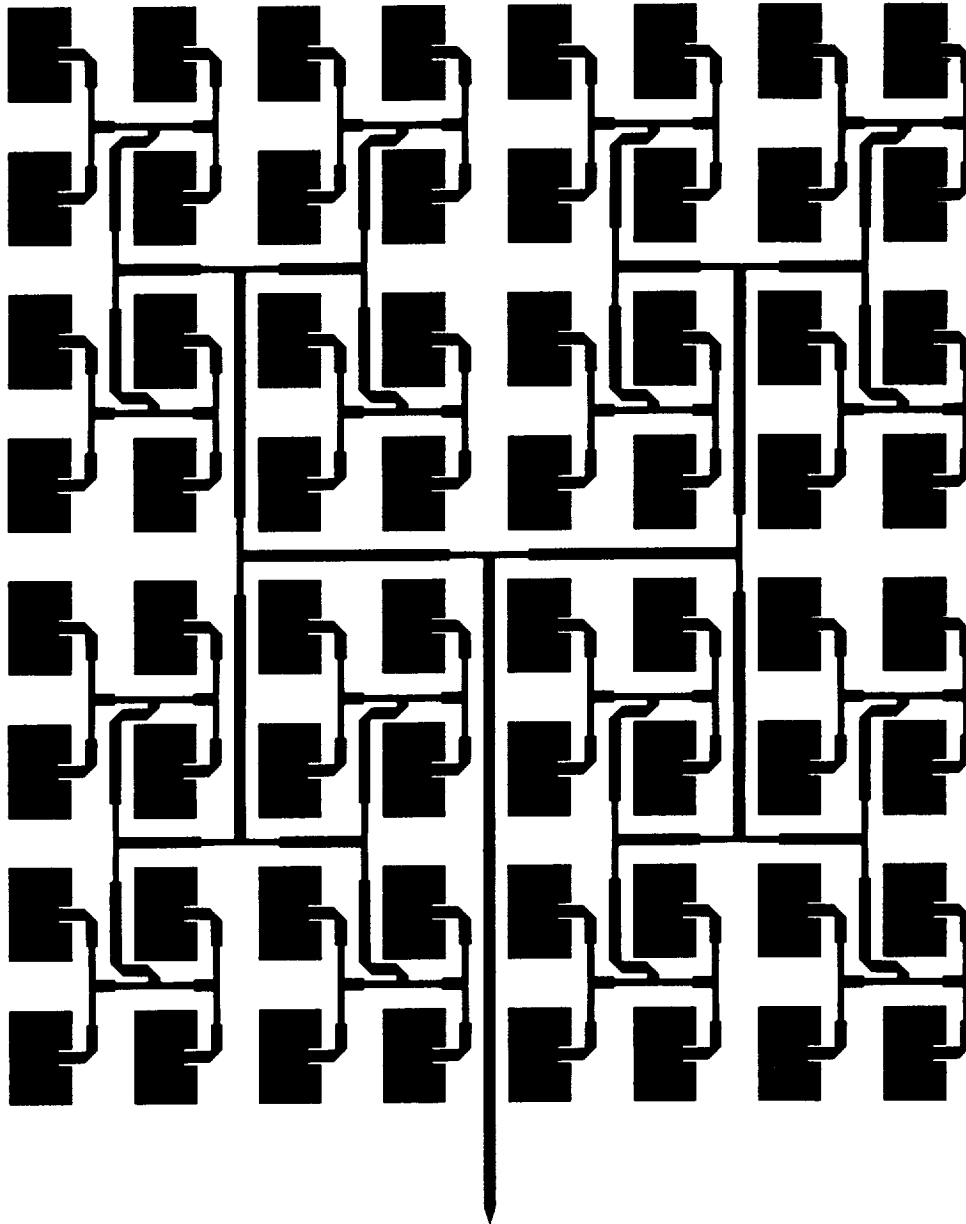
Figure 5-8. Mask of the 8x8 Sub-Array Shown Actual Size
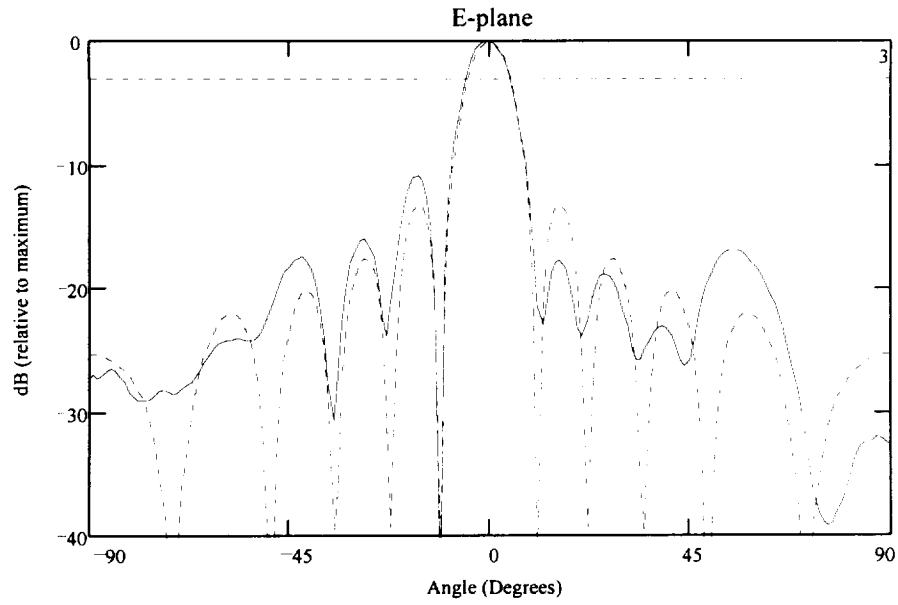
(A)
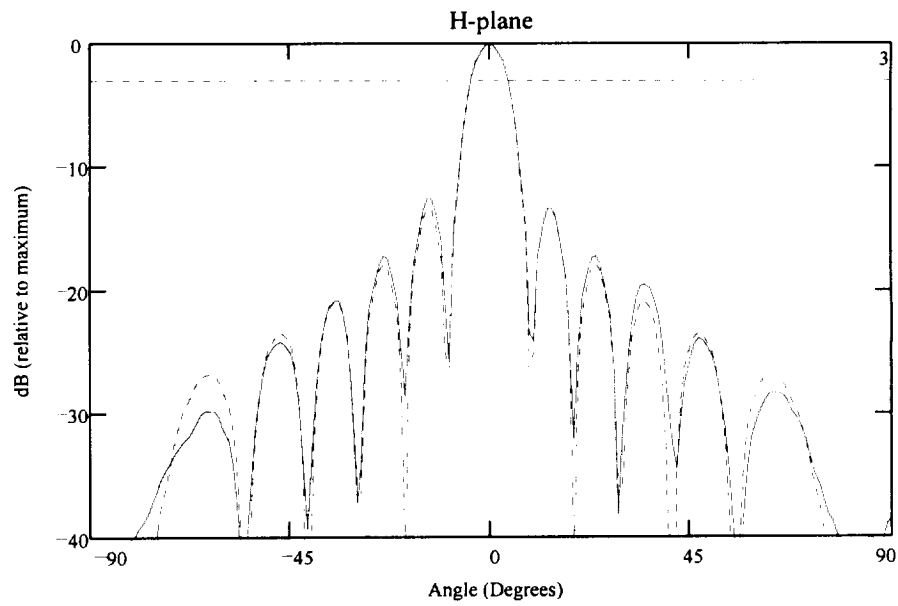
(B)

Figure 5-9. (A) E-plane and (B) H-Plane Patterns
for the 8x8 Sub-Array at 12GHz
— Measured, ---- Theoretical

S11   log MAG
REF 0.0 dB
1   10.0 dB/
V   -25.481 dB

hp

C

MARKER 1
    11.98 GHz

1→

|← ———————— Ku Band ————→

START   11.500000000 GHz
STOP   13.000000000 GHz
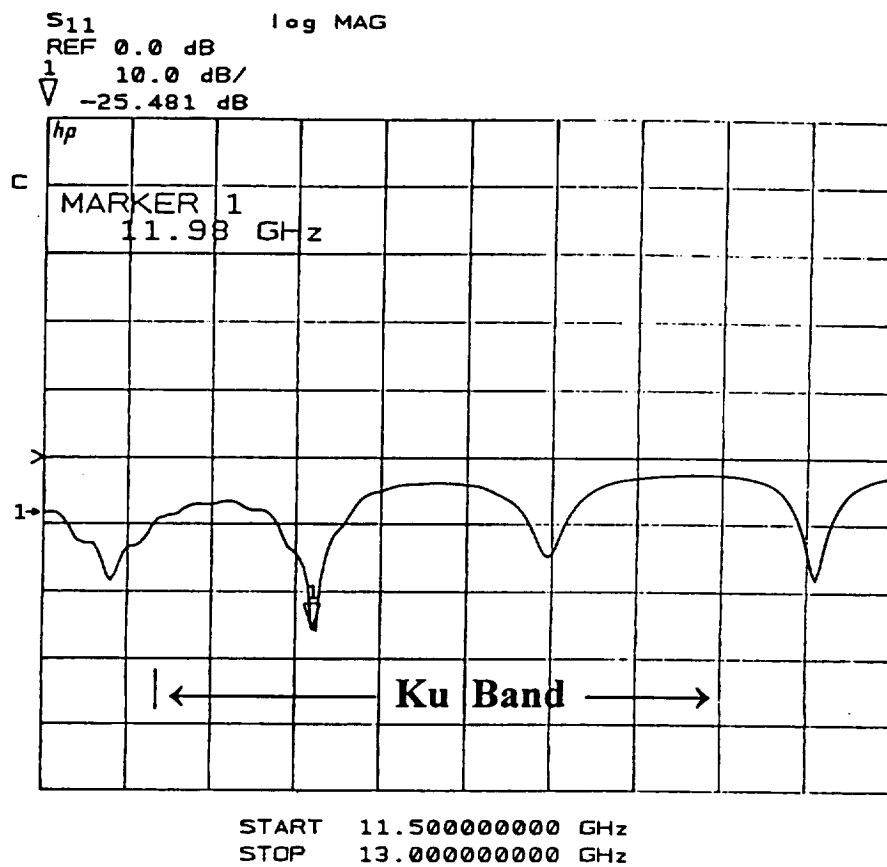
Figure 5-10. Reflection Coefficient -vs- Frequency for Modified 8x8 Sub-Array

S11   log MAG
REF 0.0 dB
      10.0 dB/

START   11.500000000 GHz
STOP   13.000000000 GHz
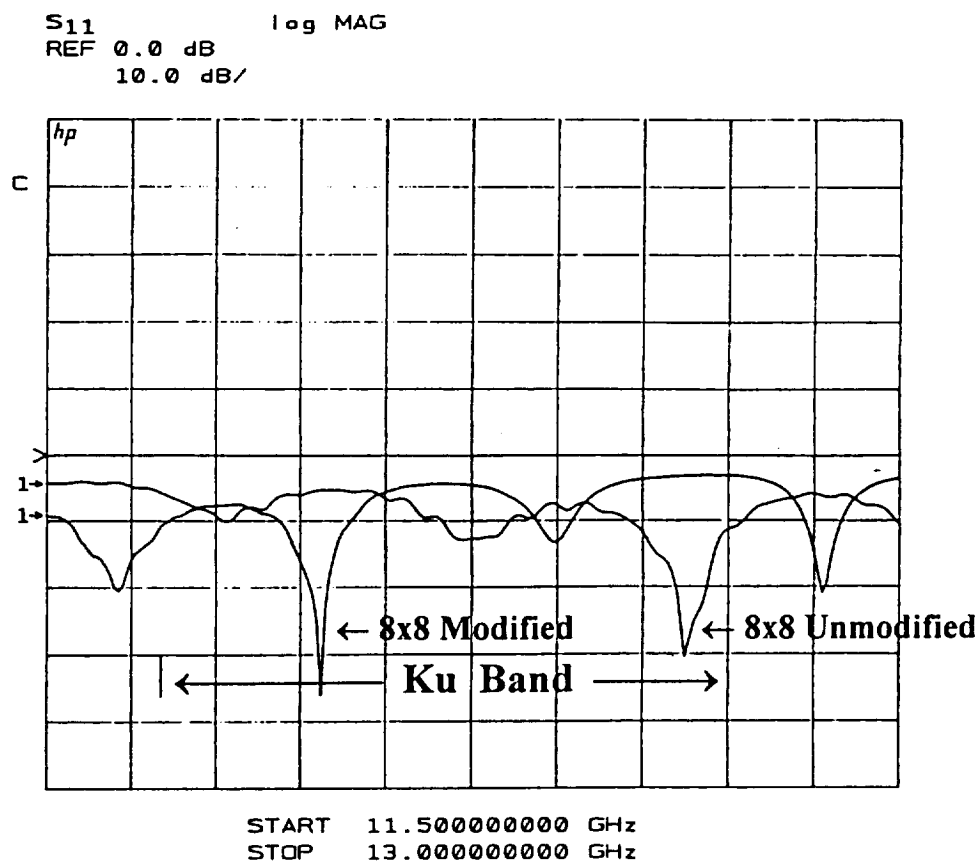
Figure 5-11. Reflection Coefficient -vs- Frequency for Modified and Unmodified 8x8 Sub-Arrays

5.4 The 8x8 EMCP Sub-Array

In an effort to determine if the overall gain of the 8x8 sub-array could be increased without compromising the complexity of its design, a few 8x8 EMCP arrays were fabricated. These arrays were constructed by simply covering the 8x8 sub-array, studied previously in this chapter, with a layer of parasitic patches separated by a dielectric superstrate. According to [2], [8] there is only a small range of superstrate

thickness' that cause an increase in gain. This range is roughly $0.3\lambda_0 \leq s \leq 0.5\lambda_0$, where s is the separation between the parasitic patches and the fed patches (superstrate thickness).

At an operating frequency of 12GHz the free space wavelength is 984mil (2.5cm). This corresponds to a superstrate thickness range of 295mil $\leq s \leq$ 492mil, or roughly 1/4in $\leq s \leq$ 1/2in. At the time of this thesis research the only suitable material available at NASA Lewis was an inexpensive styrofoam spacer ($\varepsilon_r \approx 1$) that came in 1/8in thick sheets. This limited the number of trials to three (3). One EMCP array was made with a superstrate thickness of 1/4in (250mil) a second with a 3/8in (375mil) thick superstrate and a third with a 1/2in (500mil) thick superstrate.

The H-plane patterns of the three EMCP arrays are shown in figure 5-12 with respect to the non-EMCP array. The 8x8 EMCP array with a superstrate thickness of 500mil increased the overall gain by approximately 1dB with a first sidelobe suppression greater than 3dB. Therefore, an increase in gain was attainable for the 8x8 sub-array without adding to the complexity of the design. This principle will be tested in the next section when a 16x16 EMCP array will be fabricated using four of these 8x8 EMCP sub-arrays with a superstrate thickness of 500mil.
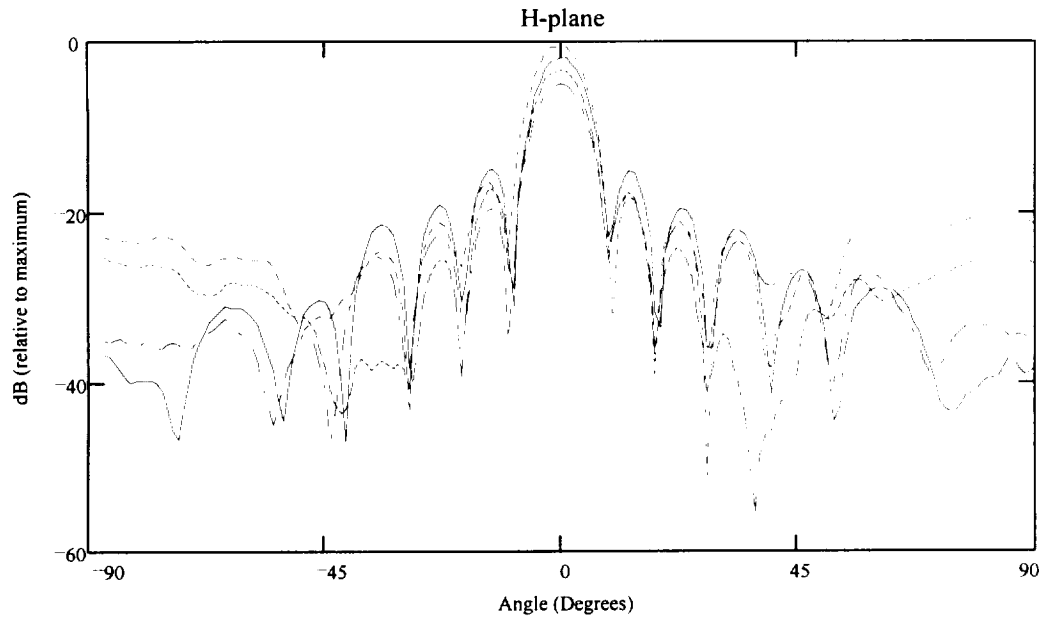
H-plane

Figure 5-12. H-plane Patterns for an (—)8x8 non-EMCP Array and Three 8x8 EMCP
Arrays with Superstrate Thickness' of (——) 500mil, (---) 375mil, and (----) 250mil

5.5 The 16x16 Array

This array was fabricated using four of the modified 8x8 sub-arrays designed to

operate at 12GHz, discussed at length in section 5-3. At the time of this thesis the photo-

etcing equipment available at NASA Lewis was incapable of etching any circuit board

larger than 7in × 7in. This is very close to the size of one 8x8 sub-array. Therefore, four

sub-arrays were etched separately and fed by an external microstrip feed network. The

external network shares the same ground plane as the sub-arrays but faces in the opposite

direction. Energy is coupled from the external network to the sub-arrays through a small

aperture cut into the ground plane, illustrated in figure 5-13.

16x16 Array

Figure 5-13. Exploded View of an Aperture Coupled Transition for the 16x16 Array

5.5.1 Measured Operating Characteristics of the 16x16 Array

The E-plane and H-plane patterns of the 16x16 array are shown in figures 5-14

(A) and (B) respectively. From these figures the 3dB beamwidth was determined to be 6°

in the E-plane and 5° in the H-plane. The gain was calculated, by the method mentioned
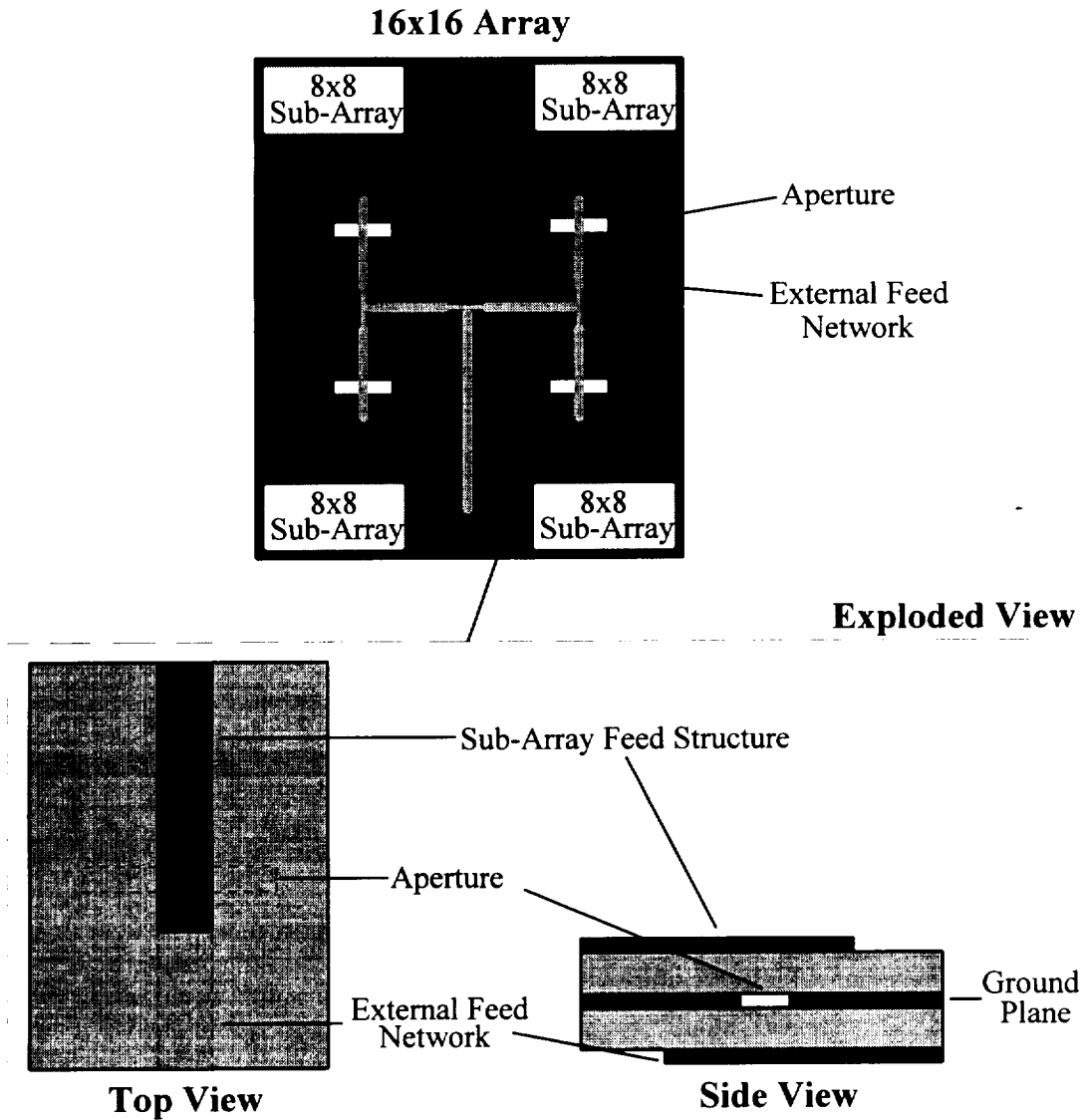
in section 4.4.2, to be 26dB. An estimate of the gain was also made by comparing the

carrier to noise ratio (C/N) of one signal received by both the 16x16 array and a NASA

Lewis 5m dish. An R.S.I. #500KS 5m dish with a gain of 53.6dB was positioned to

receive a typical Ku band television signal. The signal in question was channel 97

horizontal (12.18GHz) transmitted from the ANIK-E1 satellite (azimuth = 215.89°,

elevation = 35.65°, polarization = 81.5° from Cleveland, Ohio). The carrier power to

noise power ratio was determined from a spectrum analyzer to be roughly 45dB for the

dish. When the dish was replaced by the array the carrier to noise ratio was reduced to

19dB. This is a difference of 26dB. This difference when subtracted from the gain of the

dish results in an estimate for the array. When calculated this gain estimate is 27.6dB,

which seems to corroborate the value calculated from the method mentioned in section

4.4.2.

The size of the 16x16 array also prevented it from being connected to the network

analyzer. Therefore, the operating bandwidth could not be accurately determined and is

not given here. However, it would be reasonable to assume that the bandwidth is at least

that of the 8x8 sub-array which is 1.3%.

Studies on 16x16 EMCP arrays showed no improvement on antenna gain over the

non-EMCP array. Due to the limited amount of superstrate material only two thickness'

were tested. Therefore, more tests would have to be conducted before a conclusion can

be made about the effects parasitic patches have on antenna gain for this 16x16 array.
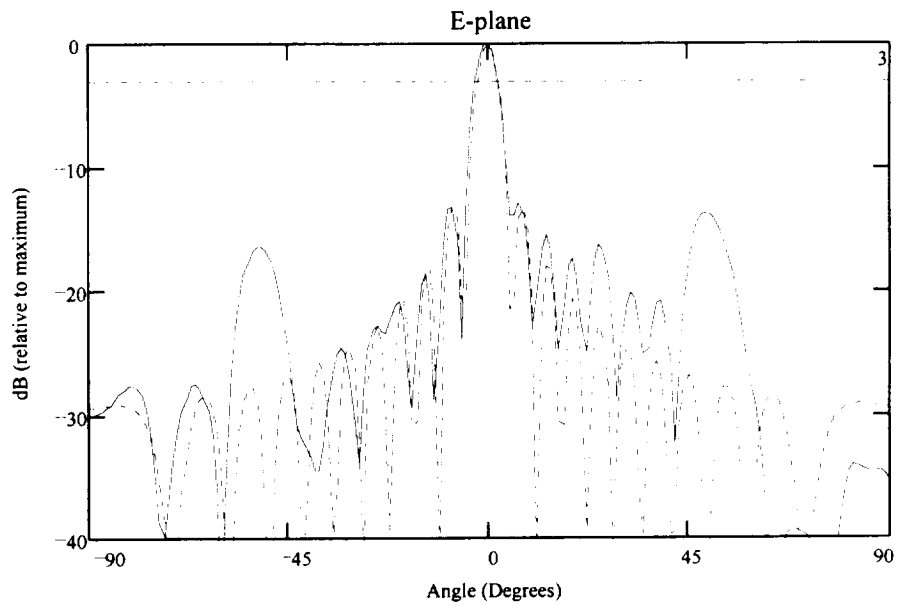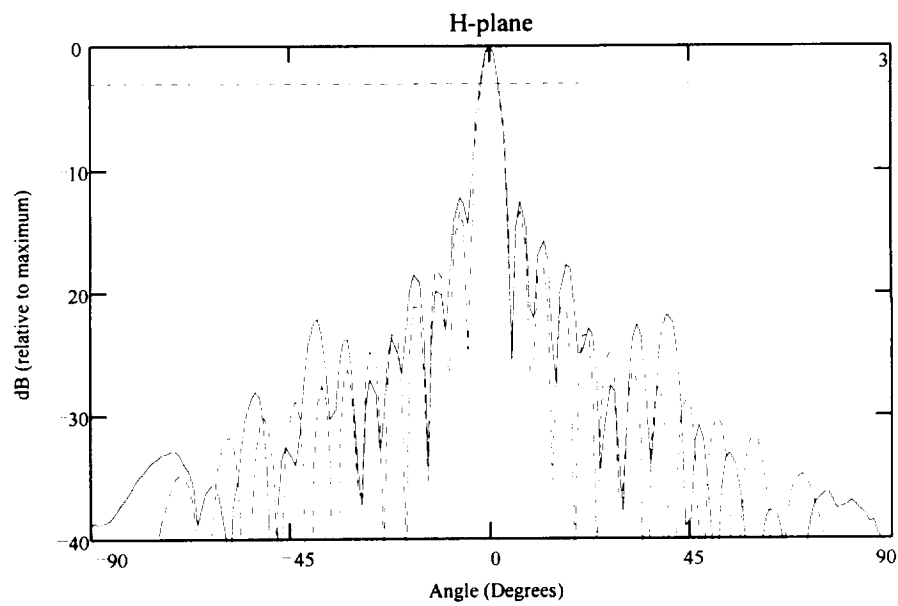
Figure 5-14 (A) E-plane and (B) H-Plane Patterns
for the 16x16 Array at 12GHz
— Measured, ---- Theoretical

5.6 Chapter Summary

This chapter presented the measured operating characteristics of the 2x2, 4x4, and 8x8 sub-arrays in addition to the 16x16 array. Specifically, these operating characteristics were, the E-plane and H-plane radiation measurements, the 3dB beamwidth in each plane, the antenna gain, and finally, the bandwidth.

Section 5.2 indicated that the center frequency of the 4x4 sub-array was higher than the 2x2 sub-array. This trend continued when an 8x8 sub-array was fabricated using the same patch dimensions and feed network used in the 2x2 and 4x4 sub-arrays. A second 8x8 sub-array was then redesigned with the appropriate modifications made in order for it to operate at 12GHz. This same array was then used to make three EMCP arrays. EMCP arrays were made in order to determine if the gain could be increased without compromising its design complexity. It was found that an 8x8 EMCP array with a superstrate thickness of 500mil was able to increase the gain by 1dB.

The largest array tested in this thesis was the 16x16 array. It had an antenna gain of about 26dB and an operating bandwidth estimated at less than 1.3%. Its 3dB beamwidth was 6° in the E-plane and 5° in the H-plane. Because of the size of this array it was impossible to fabricate all 256 patches on the same substrate. Therefore, four 8x8 sub-arrays were fabricated separately and connected by an external feed network.

Chapter 6

CONCLUSIONS AND FUTURE RESEARCH

6.1 Chapter Summaries

The first chapter of this thesis began with an introduction to the microstrip patch antenna. Some advantages and disadvantages associated with a single radiating element were then presented. Microstrip antennas were first studied because of how simple it was to fabricate radiating elements on the same circuit board as other microwave networks. This ultimately could reduce the cost and size of many communications packages. Unfortunately, studies also revealed that the operating characteristics of single patches were not optimum. Problems such as narrow bandwidth, wide beamwidth, and low antenna gain were common.

The first chapter then proceeds to introduce some methods that have been developed for improving these characteristics. Most of these methods required additional patches which obviously increase the size of an antenna. These additional patches can be either stacked on top or placed in the same plane as a main fed patch. Whether or not the added patches are fed or parasitic can also have an improved effect on an antenna's operating characteristics. Other ways to improve the characteristics of an antenna

68

included methods that alter the permittivity of the substrate. Usually these methods increased the complexity of the antenna.

Also included in the first chapter was a brief description of NASA Lewis' fabrication process used for manufacturing of microstrip networks. This process was mentioned in order to describe the problems associated with fabricating any microstrip network with physical dimensions greater than 7in × 7in. This problem was encountered in chapter five when a 16x16 array was designed. The physical dimensions of this array were much greater than 7in × 7in causing a slight modification in its design.

Chapter two presented previous research made on microstrip antennas. Single patches were mentioned to have a gain as low as 5dB and a bandwidth as narrow as 2.5%. Research on different antenna geometries was then described. These antennas included small arrays and EMCP antennas. The improvements for each type of geometry was then given.

The third chapter began with an illustration of the principle of pattern multiplication. This principle states that the radiation pattern of a homogeneous antenna array (an array made from identical elements) is simply the product of the pattern from a single element and the array factor. The array factor is dependent on the number of elements, the spacing in between elements, and the amplitude and phase of the excitation currents supplied to each element. It is the array factor that causes large increases in antenna gain for antenna arrays.

Chapter three then proceeded to calculate a downlink power budget in order to estimate the gain required for a typical DBS satellite receiving antenna. This value was

used to estimate the number of microstrip patches needed to form an array with the same

gain. In order to determine the number of patches needed as well as the spacing between

each patch a program called PCAAD was used. This program, developed by David

Pozar, can estimate the radiation pattern and directivity of many microstrip arrays. From

this program it was determined that a microstrip array made from just 256 patches might

be sufficient. This array would eventually be the largest array studied in this thesis.

The fourth chapter marked the beginning of the actual experimental research made

on microstrip antenna arrays. This chapter primarily dealt with the problem of choosing

an appropriate substrate material. Once this material was chosen experimental research

was made on single patches. Specifically, the size, shape, and feed point of a single

microstrip patch were all optimized. This chapter also presented a description of each

laboratory facility available at NASA Lewis used for evaluating the operating

characteristics of antennas.

Finally, chapter five presented all of the measured characteristics for the antenna

arrays researched in this thesis. The 2x2 and 4x4 sub-array's were made of the single

patches that were optimized to operate close to 12.45GHz, mentioned in chapter four. In

order to tune the operating frequency down to 12GHz a different size patch was used for

the construction of the 8x8 sub-array and the larger 16x16 array. The operating

characteristics of the 16x16 array were measured to have an antenna gain of 26dB, a

bandwidth of at least 1.3%, and an average 3dB beamwidth of 5° in both planes.

Including all of the structural support material the overall size of the 16x16 array

measured about 12in × 18in × 1in.

The characteristics of this array do not make it highly compatible with DBS television reception, due mainly to its limited bandwidth. At a rated bandwidth of 1.3% this translates to an acceptable reception of at most 2 (two) television channels. However, for smaller data and voice channels the number of quality channels received would be much greater. In order to improve the characteristics of this array a few topics of suggested research are given in the next section.

6.2 Topics of Related Research

Two areas of research exist for increasing the number of television channels received by the 16x16 array studied in this thesis. The first area involves tuning its narrow 1.3% bandwidth over a large band of frequencies. Referring to the discussion in chapter two, the operating frequency of a single microstrip patch antenna can be changed by simply altering the permittivity of its substrate. A tuning range of up to 20% has been accomplished for a single patch antenna. However, studies on the effects a change in substrate permittivity has on larger microstrip arrays are limited. Therefore, research on incorporating permittivity altering techniques for large 16x16 arrays could be made.

A second area of research for increasing the number of received television channels involves increasing its overall bandwidth. This could be accomplished by constructing the array with a layer of parasitic patches separated by less than $0.15\lambda_0$ from the fed array layer. This range of superstrate thickness for an EMCP type array, studied by [2] and [8], typically resulted in an increase in overall bandwidth. However, their studies were also limited to only single patches and small arrays. Research on large

16x16 EMCP arrays with superstrate thickness' conducive to an increase in bandwidth could also be made.

In order to improve the carrier to noise ratio of any received television signal the gain of the 16x16 array should be increased. As mentioned in section 5.4 and 5.5, an attempt to increase the gain of the 8x8 sub-array and the 16x16 array was made by placing parasitic patches on top of the fed array layer but with a superstrate thickness in the range $0.3\lambda_0 < s < 0.5\lambda_0$. However, due to the insufficient amount of superstrate material present at NASA Lewis a thorough study on gain enhancement was impossible. Therefore, continued research in this area could be made as well.

Finally, A large motivation behind the research conducted in this thesis was to determine if a cheaper more practical antenna could be made to compete with existing satellite receiving antennas. Most satellite receiving antennas are parabolic reflectors that require mechanical motors to steer their main beam. If the amplitude and phase of the excitation current fed to each patch in the 16x16 array can be controlled electronically then the main beam of the antenna can also be controlled. This type of antenna is usually called a phased array antenna. The ability to make a lightweight, flat, and electronically steerable satellite receiving antenna would reduce the set up time and pointing loss associated with most parabolic reflectors. If improvements on the bandwidth of the 16x16 array can be successfully made then research into microstrip phased array antennas would be the most logical choice.

REFERENCES

[1]   K.F. Lee and J.S. Dahele, "Characteristics of Microstrip Patch Antennas and Some Methods of Improving Frequency Agility and Bandwidth", Chp. 3 in James, J.R. and Hall, P.S. (Ed): *Handbook of Microstrip Antennas*, Peter Peregrinius, pp. 111-217, 1989.

[2]   R.Q. Lee, K.F. Lee, and J. Bobinchak, "Characteristics of a Two-Layer Electromagnetically Coupled Rectangular Patch Antenna", *Electronics Letters*, Vol. 23, No. 20, pp. 1070-1073, 1987.

[3]   A.A. Efanov and H.W. Thim, "Corporate-Fed 2x2 Planar Microstrip Patch Sub-Array for the 35GHz Band", *Antennas and Propagation Magazine*, Vol. 37, No. 5, pp. 49-51, October 1995.

[4]   Thomas Laverghetta, *Microwave Materials and Fabrication Techniques -2nd edition*, Artech House, Inc., Section 4.3.2 "Rubyliths", pp. 91-93, 1991.

[5]   Y.T. Lo, D. Solomon, and W.F. Richards, "Theory and Experiment on Microstrip Antennas", *IEEE Transactions on Antennas and Propagation*, Vol. AP-27, No.2, pp. 137-145, March 1979.

[6]   K.F. Lee, "Microstrip Patch Antennas - Basic Properties and Some Recent

Advances", *Journal of Atmospheric and Terrestrial Physics*, Vol. 51,

pp. 811-818, 1989.

[7]   K.F. Lee, R.Q. Lee, and T. Talty, "Microstrip Subarray with Coplanar and

Stacked Parasitic Elements", *Electronics Letters*, Vol. 26, pp. 668-669, 1990.

[8]   R.Q. Lee and K.F. Lee, "Gain Enhancement of Microstrip Antennas with

Overlaying Parasitic Directors", *Electronics Letters*, Vol. 24, pp. 656-658, 1988.

[9]   P. Bhartia and I.J. Bahl, "A Frequency Agile Microstrip Antenna", *IEEE AP-S

International Symposium*, pp. 304-307, 1982.

[10]   D.H. Schaubert, F.G. Farrar, A.R. Sindoris, and S.T. Hayes, "Microstrip Antenna

with Frequency Agility and Polarization Diversity", *IEEE Transactions on

Antennas and Propagation*, Vol. 29, pp. 118-123, 1981.

[11]   M.T. Ma, *Theory and Application of Antenna Arrays*, Wiley-Interscience

Publication, Section 1.1 "Radiation Characteristics to be Studied", pp. 2-4, 1974.

[12]   Reference [11], Section 3.1 "Rectangular Arrays", pp. 188-191, 1974.

[13]   T. Pratt and C.W. Bostian, *Satellite Communications*, John Wiley & Sons, Section 4.1 "Basic Transmission Theory", pp. 108-113, 1986.

[14]   Reference [13], Section 4.2 "System Noise Temperature and G/T Ratio", pp. 113-119, 1986.

[15]   Reference [13], Section 11.4 "Direct Broadcast Satellites", pp. 435-436, 1986.

[16]   Reference [13], Section 11.2 "Satellite Television Receivers", pp.433-434, 1986.

[17]   Rogers Corporation, Microwave Materials Division, *RT/duroid Microwave Laminates Design Guide*, 1988.

[18]   P. Bhartia, K.V.S. Rao, and R.S. Tomar, *Millimeter-Wave Microstrip and Printed Circuit Antennas*, Artech House, Section 3.2.1 "Surface-Wave Excitation", pp. 49-51, 1991.

[19]   Reference [18], Section 3.2.3 "Dielectric Loss and Copper Loss", pp. 52-55, 1991.

[20]   T. Huynh, K.F. Lee, and R.Q. Lee, "Cross Polarization Characteristics of Rectangular Patch Antennas", *Electronics Letters*, Vol. 24, pp. 463-464, 1988.

[21]   David M. Pozar, *Microwave Engineering*, Addison-Wesley, Section 5.4, "The

Scattering Matrix", pp. 220-231, 1990.